



## Nanocellulose and PEDOT:PSS composites and their applications

Robert Brooke, Makara Lay, Karishma Jain, Hugo Francon, Mehmet Girayhan Say, Dagmawi Belaineh, Xin Wang, Karl M. O. Håkansson, Lars Wågberg, Isak Engquist, Jesper Edberg & Magnus Berggren

To cite this article: Robert Brooke, Makara Lay, Karishma Jain, Hugo Francon, Mehmet Girayhan Say, Dagmawi Belaineh, Xin Wang, Karl M. O. Håkansson, Lars Wågberg, Isak Engquist, Jesper Edberg & Magnus Berggren (2023) Nanocellulose and PEDOT:PSS composites and their applications, Polymer Reviews, 63:2, 437-477, DOI: [10.1080/15583724.2022.2106491](https://doi.org/10.1080/15583724.2022.2106491)

To link to this article: <https://doi.org/10.1080/15583724.2022.2106491>



© 2022 The Author(s). Published with license by Taylor & Francis Group, LLC



Published online: 16 Aug 2022.



Submit your article to this journal [↗](#)



Article views: 5699



View related articles [↗](#)






View Crossmark data [↗](#)



Citing articles: 4 View citing articles [↗](#)

## Nanocellulose and PEDOT:PSS composites and their applications

Robert Brooke<sup>a</sup> , Makara Lay<sup>b,c</sup> , Karishma Jain<sup>d</sup>, Hugo Francon<sup>d</sup>, Mehmet Girayhan Say<sup>b</sup>, Dagmawi Belaineh<sup>a</sup>, Xin Wang<sup>a</sup>, Karl M. O. Håkansson<sup>e</sup>, Lars Wågberg<sup>d,f</sup>, Isak Engquist<sup>b,g</sup>, Jesper Edberg<sup>a</sup> , and Magnus Berggren<sup>b,g</sup>

<sup>a</sup>Digital Systems, Smart Hardware, Bio- and Organic Electronics, RISE Research Institutes of Sweden, Norrköping, Sweden; <sup>b</sup>Department of Science and Technology, Laboratory of Organic Electronics, Linköping University, Norrköping, Sweden; <sup>c</sup>INM- Leibniz Institute for New Materials, Saarbrücken, Germany; <sup>d</sup>Department of Fibre and Polymer Technology, KTH Royal Institute of Technology, Stockholm, Sweden; <sup>e</sup>Bioeconomy & Health, RISE Research Institutes of Sweden, Stockholm, Sweden; <sup>f</sup>Department of Fibre and Polymer Technology, Wallenberg Wood Science Center, KTH Royal Institute of Technology, Stockholm, Sweden; <sup>g</sup>Wallenberg Wood Science Center, Linköping University, Norrköping, Sweden

### ABSTRACT

The need for achieving sustainable technologies has encouraged research on renewable and biodegradable materials for novel products that are clean, green, and environmentally friendly. Nanocellulose (NC) has many attractive properties such as high mechanical strength and flexibility, large specific surface area, in addition to possessing good wet stability and resistance to tough chemical environments. NC has also been shown to easily integrate with other materials to form composites. By combining it with conductive and electroactive materials, many of the advantageous properties of NC can be transferred to the resulting composites. Conductive polymers, in particular poly(3,4-ethylenedioxythiophene):poly(styrene sulfonate) (PEDOT:PSS), have been successfully combined with cellulose derivatives where suspensions of NC particles and colloids of PEDOT:PSS are made to interact at a molecular level. Alternatively, different polymerization techniques have been used to coat the cellulose fibrils. When processed in liquid form, the resulting mixture can be used as a conductive ink. This review outlines the preparation of NC/PEDOT:PSS composites and their fabrication in the form of electronic nanopapers, filaments, and conductive aerogels. We also discuss the molecular interaction between NC and PEDOT:PSS and the factors that affect the bonding properties. Finally, we address their potential applications in energy storage and harvesting, sensors, actuators, and bioelectronics.

### ARTICLE HISTORY

Received 4 March 2022  
Accepted 21 July 2022

### KEYWORDS

PEDOT; nanocellulose; composites; cellulose; conductive polymers

**CONTACT** Jesper Edberg  [jesper.edberg@ri.se](mailto:jesper.edberg@ri.se)  Digital Systems, Smart Hardware, Bio- and Organic Electronics, RISE Research Institutes of Sweden, Norrköping, Sweden

This article has been republished with minor changes. These changes do not impact the academic content of the article.

© 2022 The Author(s). Published with license by Taylor & Francis Group, LLC

This is an Open Access article distributed under the terms of the Creative Commons Attribution-NonCommercial-NoDerivatives License (<http://creativecommons.org/licenses/by-nc-nd/4.0/>), which permits non-commercial re-use, distribution, and reproduction in any medium, provided the original work is properly cited, and is not altered, transformed, or built upon in any way.

## 1. Introduction

The demand for advanced applications toward green electronics and clean energy in today's society to support the United Nations sustainability goals will require the improvement of materials performance, selection, and fabrication technology. Organic electronics have several advantages as compared to inorganic materials such as being lightweight, mechanically flexible, and environmentally friendly; thereby extending opportunity to develop devices using low-cost fabrication techniques such as coating or printing. Printed and flexible electronics created from organic electronic materials offer the manufacturers and developers the potential advantages of being cost-effective, light weight, economic and environmentally friendly.<sup>[1]</sup> The organic electronic materials in the form of conductive inks with active materials such as carbon nanotubes, graphene, graphene oxide, silver (usually nanoparticle or microparticle ink), and conductive polymers have witnessed spectacular growth in printed electronics such as display technologies, consumer electronics, energy storage, conversion and harvesting, flexible and wearable electronics, biosensors, smart packaging, and body-integrated electronics in healthcare systems.<sup>[2]</sup> However, these inks, for instance carbon-based inks, often have rheological issues (low viscosity), low surface tension, solubility, and wettability which require the addition of hazardous solvents and binder materials to make them suitable for printing technology.<sup>[3,4]</sup> Nanocelluloses (NCs), have a number of interesting properties such as high flexibility, good mechanical properties, optical transparency, and good rheological properties that makes it well-suited for use in printed and electronic applications in addition to being sustainable and environmentally friendly.<sup>[5,6]</sup> NCs have been used as substrates for energy harvesting devices, actuators, and sensors<sup>[7]</sup> in addition to provide a template for conducting materials to form conductive inks for use in the electronics industry owing to its enhanced solubility, conductivity, and flexibility.<sup>[8]</sup> Unlike other conductive inks that usually possess low viscosity and promote “coffee-rings” during the drying process, NC-based inks suppress such coffee-ring effects due to the anisotropic Brownian motion of its particles to the periphery of the droplet.<sup>[9]</sup> Due to the anisotropy of the NCs, their strong interaction with water and their surface charge properties they will form volume spanning arrested states (VASS) and hydrogels at low solids contents.<sup>[10,11]</sup> These structures have also been shown to have shear-thinning properties.<sup>[12]</sup> The viscosity of NC dispersions can be modified by, shortening the NCs, a surface modification and/or water evaporation. Therefore, NC combined with conducting materials can produce high quality electrically conducting inks which enable the fabrication of a wide range of electronic components through spray, inkjet, screen and 3D printings, and coating processes.

Composites of NC and conducting materials such as metals<sup>[13]</sup>, Mxene<sup>[14]</sup>, and carbon-based materials<sup>[15–17]</sup> can be prepared by a blending method in which the charge-transfer and strength of the individual components are controlled by the physical interaction between the blended components.<sup>[18]</sup> NC-conductive polymer composites can also be created via another avenue which involves *in situ* polymerization. Composites created through this synthesis route include NC and polypyrrole<sup>[19,20]</sup>, polyaniline,<sup>[21,22]</sup> and poly(3,4-ethylenedioxythiophene) (PEDOT) and its derivatives<sup>[23–27]</sup>. Device fabrication from NC composites and their emerging applications were recently reviewed<sup>[18,28,29]</sup>.

Among these composites, NC and PEDOT:poly(styrene sulfonate)(PSS) is the most desirable conductive ink for commercialization due to materials availability, solubility, stability, processibility, and its electrical conductivity.<sup>[30]</sup> These conductive inks can be used for printed and flexible electronics<sup>[27]</sup> or extruded conductive filaments for electronic textile applications.<sup>[31]</sup>

Within this report, we present an overview of NC and PEDOT:PSS composite research. We provide a fundamental aspect of NC/PEDOT:PSS composites and the techniques and processes that are used to form electroactive inks, nanopapers, man-made filaments, and aerogels. Finally, we discuss the potential applications of these functional materials in energy storage, energy harvesting, sensors, actuators, and bioelectronics.

## 2. Materials

### 2.1. Cellulose

Cellulose, the most abundant biopolymer that exists in nature, is a linear organic polysaccharide consisting of  $\beta$ -1,4 linkages of anhydroglucose. The structure of cellulose is shown in Fig. 1. In nature, plants and algae utilize cellulose as a structural component in their cell walls while some bacteria use cellulose to create biofilms. Humans have exploited cellulosic materials for their own uses with cellulose being a major component in materials such as paper, cotton, wood, and hemp to name a few. Cellulose research has therefore been an extensive field to improve and invent new materials and

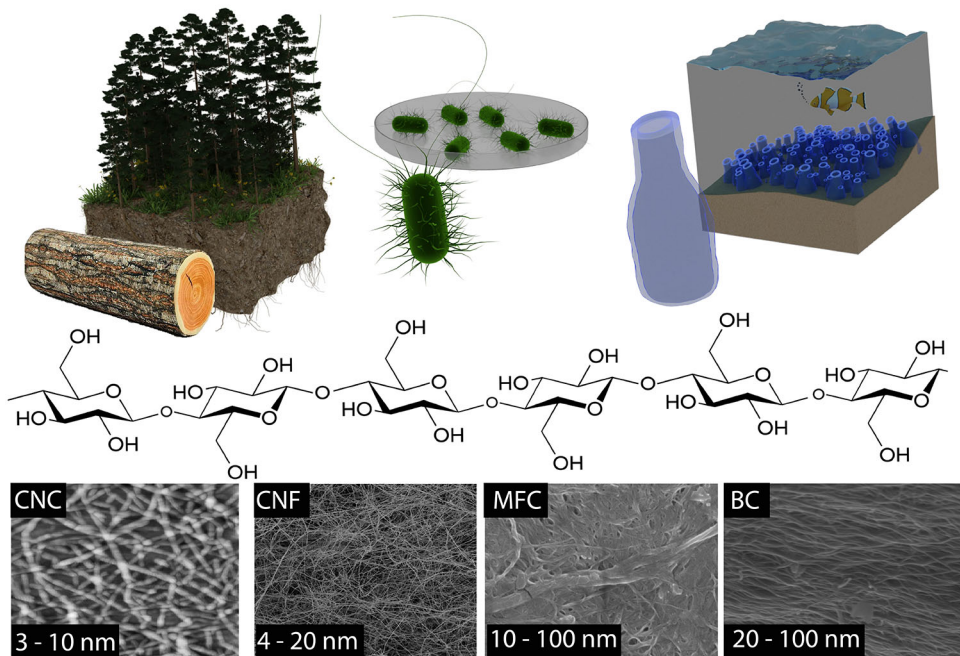


**Figure 1.** Raw materials for NC productions, type of NC and their dimension (diameter and length). Cellulose nanofibrils<sup>[34]</sup> bacterial cellulose<sup>[35]</sup>, and cellulose nanocrystals<sup>[36]</sup> images were adapted with permission.

technology.<sup>[8,32]</sup> More modern developments have included using cellulosic materials as biofuels and their development into ion exchange membranes.<sup>[33]</sup> One such modern development has been the refinery of cellulose into different sized of micro and nanofibrils, as shown in SEM images in Fig. 1. While wood fibers have been used for centuries to fabricate paper, only recently have researchers developed strategies to efficiently extract micro- and nano-fibrils from biomass and composite materials where the extracted fibrils are now being developed constantly for new applications.

## 2.2. Nanocellulose

NCs from renewable resources have received a growing interest in the last decades due to their unique structure, properties and tunability.<sup>[37]</sup> It is important to understand that NC is not one specific material, but rather the collective name of the class of particles composed of the cellulose polymer and at least one dimension in the nanoscale range. The possible variations of NCs are, therefore large, where the differences could be in size, shape, and surface chemistry which in turn would lead to differences in, for example, mechanical properties, rheology, degradation, colloidal properties, compatibility with other materials, and specific surface area (SSA). As a natural nanoscale material, NC possesses special morphology and geometrical dimensions, usually high SSA, high aspect ratio, strong inter- and intra-molecular interactions, and crystallinity.<sup>[38]</sup> The unidirectional parallel orientation of cellulose chains within the fibrils, occurring during biosynthesis and deposition, induces the formation of crystals having hydroxyl functionality on one end. The inter- and intra-molecular interactions within and between the glucan chains creates the specific properties of the material such as hydrophilicity, chirality, and ease of chemical functionalization.<sup>[39]</sup> The structure of NC materials linked to the intrinsic shape, anisotropy, surface charge/chemistry, rheology, and mechanical properties of NCs can be used to improve the performance of composite materials and development of advanced functional materials.<sup>[40]</sup>

NCs can be extracted from different raw materials mainly from forest trees, plants and agriculture residuals, tunicates or collected from cellulose-producing bacteria.<sup>[41]</sup> Wood fibers (20 – 50  $\mu\text{m}$  width and 1 – 5 mm length), extracted from trees, are arguably the most widely used cellulose fibers, since they are used in the papermaking process, regenerated cellulose manufacturing and in different hygiene products. Wood fibers consist of cellulose, hemicelluloses, and lignin in different proportions depending on species and part of the tree.<sup>[42]</sup> In papermaking, wood fibers are first delignified in the pulping and bleaching processes before the fibers are formed into paper sheets in the paper machine. The cellulose polymer is a linear biopolymer of glucan units that self assembles in nature during synthesis to a high aspect ratio and semi-crystalline nanostructure. The glucan chains are attached to each other to form fibrils, and several fibrils are bound to each other to form fibril aggregates that in turn are further combined with hemicellulose and lignin, to create the composite structure in the wood fiber. When the cellulose is liberated from the fiber wall during different processing steps to create NC materials, microfibrillated cellulose (MFC) is first formed with a broad size distribution of the particles.<sup>[43]</sup> The microfibrils can then be further converted into nanoscale building blocks, referred to as NCs.<sup>[44]</sup> These NCs can be divided into two

major versions; cellulose nano fibrils (CNFs) and cellulose nanocrystals (CNCs). Generally, the CNFs are much longer (above 1  $\mu\text{m}$ ) whereas the CNCs are shorter (100–400 nm) with a higher degree of crystallinity. In order to keep a high colloidal stability of the NCs, they are usually decorated with anionic charges, carboxylic acid groups for CNFs and sulfonic acid groups for the CNCs. There are naturally a wide variety of modification techniques available in this area but this is a valid general description of the situation today. There is still a scientific debate about the general composition of the fibrils but one accepted view is that the CNFs are made up of 36 cellulose chains, consisting of repeating units of two linked D-glucose molecules with  $\beta$  (1–4) glycosidic bonds (typically with a DP [degree of polymerization] around 10,000) and comprises crystalline and amorphous regions.<sup>[45]</sup> The dimension and degree of crystallinity of CNF depend on their sources and extraction techniques<sup>[46]</sup> and the existence of and dimensions of the amorphous regions have been highly questioned lately from high-resolution AFM and SEM techniques.<sup>[47]</sup> Most probably, the nanodimension of the fibrils and the high amount of cellulose glucan chains on the external surface of the fibrils can explain the semicrystallinity of the fibrils instead of a fringed micellar structure.

While forest or plant-based cellulose has dominated the research space and commercial market, other natural sources of cellulose exist such as bacteria-produced materials.<sup>[48]</sup> The function of cellulose originating in bacteria may differ from that of plants (UV-light and heavy metal ion protection vs. osmotic pressure protection), yet the cellulose component remains biodegradable and biocompatible with some additional advantages not seen in cellulose derived from plants. Bacterial cellulose (BC) has a higher purity compared to plant and wood cellulose due to the lack of lignin and hemicellulose which reduces purification steps.

Tunicate cellulose is a more recent discovery of naturally occurring cellulose within the animal kingdom. Tunicates, a marine invertebrate animal living either as solitary animals or in budding colonies, contain cellulose in their outer wall. Tunicate cellulose possesses an ultrafine fibrous network with a highly ordered and crystalline structure.<sup>[49]</sup> With its high aspect ratio, low density, and mechanical strength, reports have suggested its film-forming properties may surpass that of other naturally occurring cellulose.<sup>[44]</sup> Unfortunately, the production of tunicate cellulose is minimal compared to plant and BC which has undoubtedly led to its reduced take up.

The detail classification, preparation, surface modification, application, challenges, and opportunity of NCs toward industrialization can be found in recent reviews and, therefore, the full details of NCs are beyond the scope of this review.<sup>[8,44,50–52]</sup>

### **2.3. Production and properties of NCs**

The production of NC is in a state of constant development with an emphasis on the reduction of production costs and the introduction of different functional groups onto the cellulose structure.<sup>[53,54]</sup> The large SSA and the presence of a large number of hydroxyl groups within the NC structure make these nanofibers an exceptional platform for surface modification through different chemistries.<sup>[18]</sup> Different types of surface modification, e.g., before and during top-down (isolation), during and after processing,

and the introduction of different function groups on NCs have been reviewed.<sup>[8,52,55]</sup> The surface modification of NC is arguably the most important step to control the interactions between the NC nanoparticles and other materials. The introduction of surface charges, their chemistry and the surface charge density will be very important for the macroscopic properties of the CNFs dispersions such as the rheological properties and the formation of 2D and 3D materials as water is removed. These surface charges, in combination with the mechanical properties of the fibrils this will allow for an efficient combination with other materials to fabricate composite materials.<sup>[8]</sup> Depending on the type of NC and its source, different strategies are employed for its production. A top-down approach (bleaching and pulping) is used to eliminate non-cellulosic compounds such as lignin and hemicellulose.<sup>[8]</sup> Thereafter, the cellulose-rich fibers are exposed to a high-pressure mechanical treatment to produce MFC or CNF. Due to the strong interfibrillar interactions between MFC, the disintegration process is generally facilitated by different combinations of pretreatment (enzymatic or chemical treatment) and mechanical treatment. For example, prior to mechanical treatment, an acid hydrolysis treatment is used to break down amorphous regions to form CNC. If sulfuric acid is used, sulfate half esters are introduced on the CNC surfaces. For CNFs, different oxidation agents are used to introduce carboxyl groups on the fibril surfaces before fibril liberation.

Another strategy, the bottom-up approach, is used to produce BC by fermentation of low molecular weight sugars via microorganism or bacteria.<sup>[56]</sup> Although sharing similar chemistry and molecular structure, the use of different raw materials and production methods show different dimensions and structures, for instance morphology and crystallinity of NCs (Fig. 1).

### **2.3.1. Microfibrillated cellulose**

The MFC that today is commercially available usually has low charge density and consists of bundles of both cellulose micro and nanofibrils with a broad size distribution and high aspect-ratio, resulting in brush-like fibril morphology and fibrillar entanglements to form strong networks and a gel-like structure when dispersed in water.<sup>[57]</sup> The appearance of MFC is white or translucent due to the presence of large fibril bundles with sizes larger than the wavelength of the visible light spectrum. Mild mechanical pretreatment can be used to directly produce MFC from pulp cellulose; however, a chemical pretreatment is usually the preferred fabrication method

Recently, MFC with a solid content of 45 % was produced at a low energy consumption of 6.4 MWh/t, with the addition of an enzyme, using a twin-screw extrusion technique but the mechanical properties of papers made from the MFC were not impressive and the DP of the cellulose was very low.<sup>[58]</sup> It was, however, shown that commercial MFC with a rather high fraction of larger particles from fragmented fibers still could be used to prepare nanopapers with very good mechanical properties<sup>[43]</sup> and with excellent rheological properties.<sup>[57]</sup> Also, the MFC showed significant advantages in dewatering time when forming nanopapers from the dispersions.<sup>[59]</sup>

### **2.3.2. Cellulose nanofibrils**

In contrast to the procedures used for preparing MFC, a variety of functionalities can be introduced onto the surface of the fibrils within the cellulose fibers during a

pretreatment process to obtain CNF with small diameters and narrow nanofibrils size distribution.<sup>[60]</sup> Typical chemical modifications are carboxymethylation and 2,2,6,6-tetramethylpiperidine-1-oxy (TEMPO) oxidation, where carboxyl moieties are introduced onto the cellulose chains, causing an osmotic repulsion between cellulose microfibrils thus making their extraction much easier.<sup>[61]</sup> Other types of covalent modifications of the fibrils that are usually used before the homogenization of the fibers to CNFs are phosphorylation (phosphate esterification), phosphide esterification, xanthate esterification, sulfate esterification, and dicarboxylation.<sup>[52,59]</sup> After the pretreatment process, high-shear mechanical treatments by the means of, for example, high-pressure fluidizer and homogenizer, refining, grinding, and sonication can be utilized to separate the fibrils within the fiber wall. This process results in CNFs with a high aspect ratio that usually form highly entangled fibrillar networks, hydrogels, in water at 0.5–1 wt%. These hydrogels have a predominantly elastic response. The charged groups keep the nanoparticles separated due to the osmotic repulsion but due to an increased concentration of counterions in the dispersions, and friction between the CNFs, as the particle concentration is increased the free-flowing dispersions are turned into hydrogels.<sup>[57]</sup>

### **2.3.3. Cellulose nanocrystal**

CNCs are the shortest NCs with a comparably lower aspect ratio and they consist approximately of 20–40 fully extended cellulose chains regularly aligned along the longitudinal direction.<sup>[59]</sup> The CNCs generally have higher crystallinity with the low aspect ratios. Specific fields of opto-electronics have been created purely through the self-assembly of CNC materials into “liquid crystalline” structures that can be adjusted through several factors such as pH, counterions, etc. which will affect this self-assembly phenomenon.<sup>[62]</sup> To prepare CNCs, the pulp fibers are generally treated with strong acid (sulfuric acid).<sup>[63]</sup> Other acids such as muriatic acid, orthophosphoric acid, and formic acid and other reagents including ammonium persulfate and bio-enzyme have also been used.<sup>[51]</sup>

### **2.3.4. Bacterial cellulose**

BC, unlike other cellulose, is cultured under static condition using microorganisms belonging to *Gluconacetobacter xylinus*.<sup>[35,64]</sup> BC production occurs at the air–water interface, where the assembly of reticulated crystalline ribbons results in a gel or pellicle.<sup>[65]</sup> BC has high water holding capacity and a distinctive structure of the fibrous three-dimensional network in the wet state formed during synthesis.<sup>[53]</sup> Several fermentation technologies have been explored using specific fermentation media, overproducing mutant strains, using agitated, airlift, membrane, and horizontal bioreactors. Despite the use of low-cost substrates, the high capital investment and operation costs present a strong economic constraint to the industrial-scale production of BCs.<sup>[48]</sup> Extensive efforts on advanced fermentation or use of agriculture and industrial waste have been devoted to determining the scientific and technological factors for high-yield and cost-effective BC production.<sup>[66,67]</sup>

All four types of NC and their derivatives have been evaluated for their ability to be combined with other materials in composites, contributing their advantages of



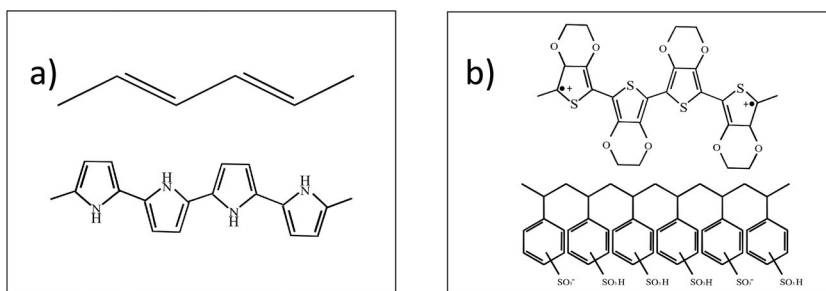


**Figure 2.** (a) Chemical structures of common conductive polymers (top) polyacetylene and (bottom) polypyrrole. (b) Chemical structures of (top) PEDOT and (bottom) PSS in their doped forms.

mechanical strength and the possibility to tailor the porosity of NC networks. While cellulose materials do not possess any conductive properties themselves, their compatibility with conductive materials allows them to be a common ingredient/substrate for conductive composites. Many types of conductive materials have been combined in composites with cellulose derivatives, including metal particles, carbonous materials, and conductive polymers. This review article focuses on the composites of conductive polymers and NC, relevant review articles on metals and carbonous material composites can be found in<sup>[68]</sup> and<sup>[17,69]</sup>, respectively.

## 2.4. Conductive polymers

Conductive polymers are an interesting, relatively new class of material that have wider range of organic compounds and molecular structures than inorganic materials and other traditional conducting materials. The field of conductive polymers was born in 1977 with the discovery of polyacetylene and the characterization of its electrical properties.<sup>[70]</sup> Recent review articles have documented their development.<sup>[71–73]</sup> The electrically conductive properties of conductive polymers originate from the delocalization of electrons from conjugated bonds throughout their chains when a dopant molecule is added or withdrawn from the structure. Since their discovery, the field of conductive polymers has expanded to include thousands of conductive polymer structures, many of which have been incorporated in many different applications in organic and printed electronics. Examples can be viewed in Fig. 2. Of the thousands of structures, PEDOT has been studied more extensively than any other due to its impressive electrical conductivity, optical and electrochromic properties, and stability in ambient conditions.<sup>[23,73–78]</sup>

### 2.4.1. Poly(3,4-ethylenedioxythiophene) (PEDOT)

PEDOT owes its impressive properties to its structure as seen in Fig. 2(b)). With the oxygens present and the phenomenon of hydrogen bonding, the PEDOT chains can be aligned and stacked in highly ordered and crystalline regions. However, the method in which PEDOT is synthesized and which dopant molecules are incorporated has a profound effect on the resultant conductive polymer properties

Of the various polymerization methods (chemical polymerization, electrochemical polymerization, and vapor phase polymerization), that have been utilized to synthesis PEDOT, chemical polymerization with the dopant PSS (and an oxidant) has achieved a water stable dispersion that can be adapted post-polymerization to adjust the properties, formulated into an ink or combined with other materials to create new composites.

#### ***2.4.2. Poly(3,4-ethylenedioxythiophene): poly(styrene sulfonate) (PEDOT:PSS)***

PEDOT:PSS has mixed ionic-electronic properties in which PEDOT acts as positive charge and insulating PSS as negative charge. The PEDOT short chain (6 – 18 repeating units) interacts with the long molecular chain of PSS by coulombic forces, allowing acceptable solubility of the conductive polymer. The morphology of a PEDOT:PSS dispersion is generally composed of a PEDOT-enriched core and a polyanion PSS shell in the form of coiled-like and randomly oriented structures. This feature limits the available charge transport pathways, leading to low conductivity properties<sup>[79]</sup> which was the case for the first synthesized PEDOT:PSS that had an electrical conductivity of approximately 10 S/cm.<sup>[70]</sup> The optimization of transport properties in conductive polymers are obtained from high carrier mobility, the efficient intra- and inter-chain transport that are linked to the degree of order and the relative stacking between the chains, and crystallinity.<sup>[72]</sup> Over the last decades, PEDOT:PSS has been extensively investigated to optimize the versatile properties via molecular or structural design, synthesis conditions, processing additives, or post-treatment. Surface and structure modification through second and/or post doping processes give a wide range of electrical conductivities ranging from  $10^{-4}$  to 103 S/cm.<sup>[80–82]</sup> Secondary dopants (such as dimethyl sulfoxide (DMSO), ethylene glycol (EG), methanol, etc.), aqueous or organic solutions of salts and acids (hydrochloric and sulfuric), or ionic liquids are used to regulate the intermolecular coupling ( $\pi$ - $\pi$  stacking) and to remove an excess PSS, leading to inducing morphological re-arrangement or phase separation.<sup>[83]</sup>

Dong and Portale used different solvents to enhance the electrical conductivity of PEDOT:PSS films. Grazing incidence wide angle X-ray scattering (GIWAXS) indicated a shortened  $\pi$ - $\pi$  stacking distance between the PEDOT molecules and the formation of both face-on and edge-on PEDOT crystallite, which helps the delocalization of the hole carrier mobility, and thus increases charge transport properties.<sup>[84]</sup> In addition, the conductivity of EG-treated PEDOT:PSS increased from 620 up to 1228 S/cm at heat-stirred temperatures of 25 °C and 90 °C, respectively, while maintaining its transmittance above 80%.<sup>[79]</sup> On the other hand, with the addition of an ionic liquid, a PEDOT:PSS film exhibited superior stretchability while maintaining its initial conductivity (1228 S/cm) under a tensile strain of 80%.<sup>[85]</sup> To date, the highest conductivity of PEDOT:PSS film can reach 4840 S/cm through  $H_2SO_4$  post-treatment.<sup>[86]</sup> As seen within this section, many approaches have been reported to improve the properties of PEDOT:PSS. This gives researchers flexibility when it comes to treatments which can become important for specific applications. Another option for researchers that is unique to PEDOT:PSS is that it can be purchased commercially as a suspension in water. One current commercial product is under the trade name of Clevios by Heraeus. The different grades such as Clevios P, Clevios PH series, Clevios PVP series, to name a few, with different

viscosity, conductivity, and optical properties are produced to meet the specific deposition technologies (screen/inkjet printing) and applications, for instance printed organic electronic or optical-electronic devices.<sup>[75]</sup> Agfa has introduced large-scale production for printing application under the trade name of Orgacon.<sup>[74]</sup>

### 3. Interaction between NC and PEDOT:PSS: fundamental aspects

Recently, the synthesis of cellulose/PEDOT:PSS nanocomposites has become significantly interesting to the scientific literature in regards to the sheer amount of reports published.<sup>[24–26,87–95]</sup> However, most of the literature focuses on applications and device characterization rather than dealing with the interactions of PEDOT and cellulose. The theoretical studies and fundamental knowledge on understanding the mechanisms and interactions between these components at nanoscale level are an important piece of the nanocomposite's investigation. In-depth fundamental research will aid researchers in understanding how the two materials are combined, which type of molecular interactions are present, and what steps can be taken to improve the composite's performance such as electronic and ionic conductivity, mechanical strength, or flexibility in addition to highlighting which applications the composite materials are most suited to. In conjunction with the development of more robust NC/PEDOT:PSS products, the fundamental interactions at the sub-micro level that dictate the performance of the devices have also been investigated based on both, experimental, with spectroscopic techniques, and theoretical, with molecular dynamics simulations.

In one study, Montibon *et al.* investigated the interactions between MFC and PEDOT:PSS (1:2.5 and 1:6 w/w ratios) at various pH and salt concentrations.<sup>[24]</sup> They reported that PEDOT (not PSS) adsorbs more on cellulose treated (hemicellulose removal) at pH 2 because charged groups of cellulose are protonated, and, therefore, charged fibrils become neutral at this pH level. However, the deprotonation of carboxylic acid in cellulose and deprotonation of PSSH to PSS<sup>-</sup> at higher pH levels contributes to negative charges on their surfaces, thus increases the electrostatic repulsion between both components, leading to lower adsorption interaction. Therefore, less amount of PSS content in PEDOT:PSS will lower the repulsion force in the system. At high salt concentrations, the adsorption of salt on the cellulose reduced diffusion and adsorption of the PEDOT:PSS, and the size of the double layer of PEDOT:PSS itself is reduced which alters the polymer diffusion. Furthermore, similar to an earlier study<sup>[96]</sup> on the interaction of polyelectrolytes with cellulose, Montibon *et al.* reported the role of ionic strength of salt concentration on screening-enhanced or screening-reduced interactions.<sup>[24]</sup> They argue that a higher salt concentration leads to a higher adsorption of PEDOT:PSS due to three reasons: (1) ionic screening effect of electrostatic interactions with the cellulose, (2) reduced size of the double layer of suspended particles which leads to a higher diffusion of PEDOT:PSS, and (3) shrinkage of the polymer at higher salt concentration leading to higher penetration into the cellulosic microstructure.

More recently, Jain *et al.*, used a quartz crystal microbalance with dissipation (QCM-D) and colloidal probe atomic force microscopy (CP-AFM) to evaluate the adsorption and adhesion of PEDOT:PSS on CNFs.<sup>[93]</sup> The result indicated that the highest adsorption mechanism of the interaction between CNF and PEDOT:PSS were obtained

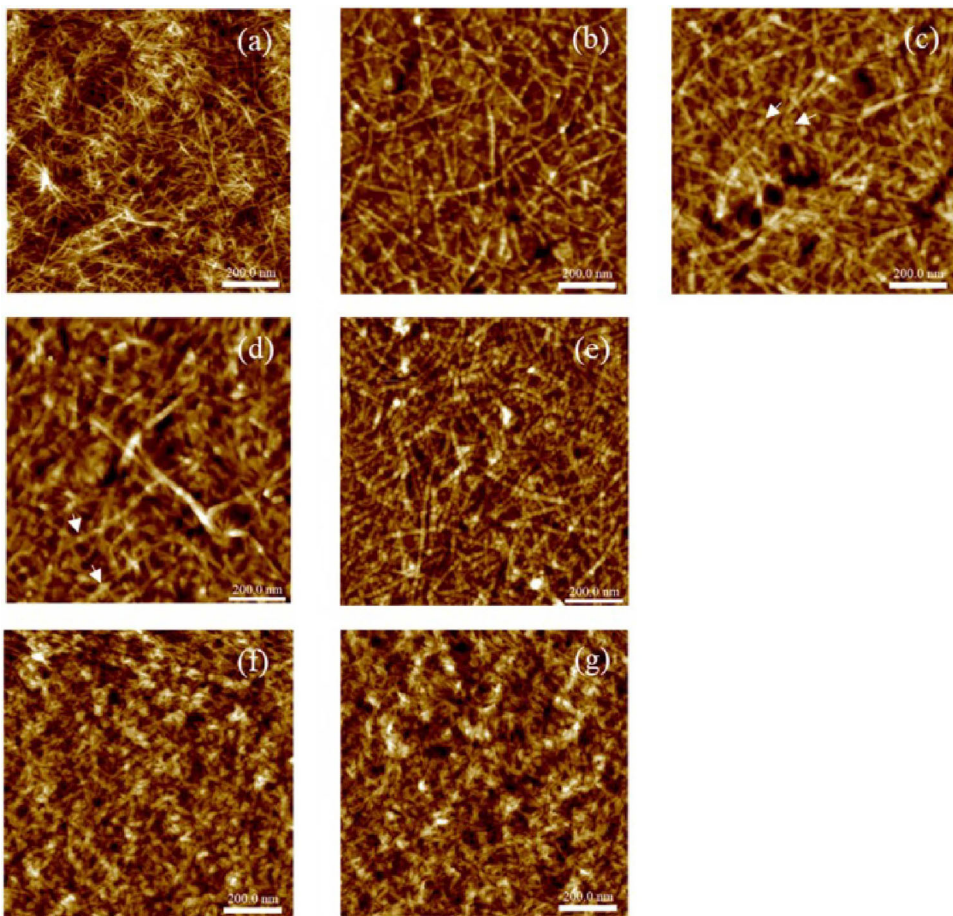


**Figure 3.** AFM height images showing (a) a CNF film, and PEDOT:PSS particles at pH 3.5, adsorbed on CNF films with (b) no added salt, (c) 10 mM added NaCl, (d) 50 mM added NaCl, (e) CNFs after ion exchange to  $\text{Ca}^{2+}$  as counterion, (f) regenerated cellulose films before adsorption, and (g) PEDOT:PSS particles at pH 3.5, adsorbed on regenerated cellulose films. Scale bar is 200 nm in each image. Reproduced with permission from Elsevier.<sup>[93]</sup>

at pH 2, at 40 °C, and high ionic strength with divalent counterions of  $\text{Ca}^{2+}$ . A bead-like structure of PEDOT:PSS particles on the CNF surface was observed from AFM (see Fig. 3), indicating a good adhesion between these two materials at the above conditions. However, they have not examined how these factors affect charge transport properties and thus conductivity of CNF/PEDOT:PSS systems.

Meanwhile, many studies have demonstrated an improvement in electrical conductivity of CNF/PEDOT:PSS films by adding high boiling point solvents as secondary dopants and/or post-treatments.<sup>[25,97]</sup> These methods have been shown to change the molecular structure of PEDOT:PSS from coiled-like and random structures to oriented structures and also to decrease the PSS insulator amount in the nanocomposites.<sup>[25,98]</sup> The reduction of negative charges on PEDOT:PSS allows PEDOT to adsorb on the NC in a well-organized shell structure along the nanofibrils. Malti *et al.* stressed that the relatively high conductivity (420 S/cm) of CNF-PEDOT:PSS films was due to the strong

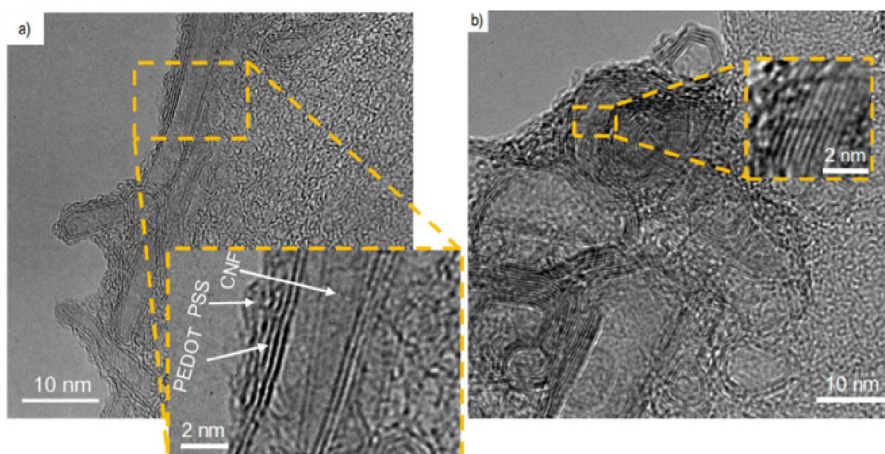


**Figure 4.** TEM image of a) PEDOT:PSS on the surface of CNF and b) highly crystalline PEDOT:PSS segregated from CNF surface. Insets show magnified images of the selected areas. Reprinted (adapted) with permission from Belaineh, D., *et al* Copyright 2021 American Chemical Society.<sup>[36]</sup>

interaction of CNF and PEDOT:PSS by van der Waals forces and the formation of  $\pi$ - $\pi$  stacking of PEDOT on CNF. They indicated that CNF acts as a template to promote self-orientation of the PEDOT chains. From WAXS and GIWAXS, they observed a random orientation of the crystalline PEDOT domains.<sup>[25]</sup> For better understanding on how PEDOT:PSS crystalline is formed on the NC surface, Belaineh *et al.* reported a comparative study between fibrillated and polymeric cellulose types mixed with PEDOT:PSS.<sup>[36]</sup> CNF and carboxymethylated cellulose (CMC) were used as templates for fibrillated and polymeric cellulose, respectively. The electrical conductivity of the film created with CNF (400 S/cm) was found to be significantly higher than that of the polymeric CMC (100 S/cm), indicating a structural role of the cellulose. They utilized nanoscopic imaging techniques to elucidate the organization of PEDOT:PSS on cellulose. This was confirmed with AFM imaging which demonstrated a unique self-assembly of PEDOT:PSS in the form of 13 nm size bead-like structures on top of cellulose fibrils. Transmission electron microscopy (TEM) (shown in Fig. 4) and a combination of GIWAXS and WAXS measurements pin-pointed a crystallographic arrangement of PEDOT with a face-on attachment on the side of cellulose fibrils.

Investigations were taken further by Mehandzhiyski *et al.*, who used coarse-grained MARTINI molecular dynamic simulations to describe the nanoscopic morphology created by the interaction of CNF and PEDOT:PSS.<sup>[99]</sup> They reported on the self-assembly of PEDOT:PSS on CNFs starting from various initial conditions. To account for the granular nature of PEDOT:PSS, the starting conditions for several models were made inhomogeneous by creating PSS<sup>-</sup>-rich and PSSH-rich regions in the simulation box. They concluded that, in general, inhomogeneous starting conditions lead to aggregated PEDOT particles on top of cellulose. However, they note that other factors such as high ionic strength, which they modeled with a high amount of Na<sup>+</sup> ions, limit the aggregation of PEDOT on cellulose due to strong electrostatic interactions. Furthermore, this computational paper predicts PEDOT stacking and orientation on cellulose which coincide with experimental investigations.

The properties of cellulose and PEDOT:PSS nanocomposites are governed by the molecular level interaction between two colloidal systems. As discussed, PEDOT:PSS has been shown to adsorb as a globular phase onto carboxymethylated CNFs when prepared from low pH aqueous dispersions. Although the nature of the interactions between cellulose and PEDOT has been under scrutiny of the research community, it is still not fully understood. It has been shown to depend on the surface properties of cellulose such as charge density, with more favorable interactions at higher charge density.<sup>[36]</sup> Several factors such as pH, ionic strength, type of celluloses, etc., were reported to control the interaction, as described above.<sup>[24,36,25,99]</sup> Different types of interactions such as H-bonding due to the presence of  $\text{-OH}$  groups on cellulose<sup>[26,100,101]</sup> and  $\pi$ - $\pi$  interactions due to amphiphilic character of cellulose<sup>[36,25,102]</sup> were suggested to be responsible for PEDOT:PSS organization on its surface. Although these studies explain the bulk level properties using different interaction forces, the framework for understanding the nanoscale forces of interaction is not available and the studies focusing on this issue are sparse. The other important factor to consider is that PEDOT:PSS is also a polyelectrolyte. Its structure, morphology, and properties will be affected significantly by changing parameters such as pH, ionic strength, and type of counterion to PEDOT. Kong *et al.*<sup>[103]</sup> and Mochizuki *et al.*<sup>[104]</sup> studied the effect of pH and ionic strength on structure and conductivity of PEDOT:PSS films. They reported the change from bipolaron to polaron state when pH of the solution is increased, thereby decreasing the conductivity of films. Modarresi *et al.* used computational microscopy simulation to study the effect of pH on the morphology of PEDOT:PSS. Their study showed that the morphology strongly depends on the pH. Crystalline PEDOT consisting of 3–4 chains is formed at pH 2.5, whereas the granular structure featuring PEDOT-rich and PSS-rich regions is observed at pH > 5.<sup>[105]</sup>

Along with pH factors, humidity can also play a significant role in effecting the cellulose/PEDOT:PSS composites. Brett *et al.* recently reported experimental data showing the effect of humidity on the conductivity of CNF/PEDOT:PSS composites with an in depth investigation into the structure using advanced neutron scattering techniques.<sup>[106]</sup> Within this work, the authors showed that humidity first has an irreversible effect before stabilizing. This is important information which could lead to pre-humidification processing steps to aid in the manufacture of stable CNF/PEDOT:PSS composites and their use in opto-electronic devices.

An important aspect governing the fundamentals of a cellulose/PEDOT:PSS nanocomposite is the procedure in which the two are combined. The following section outlines the various ways researchers have composited cellulose and PEDOT:PSS and the different results these procedures have led to.

#### 4. Preparation of NC/PEDOT:PSS nanocomposite

Composite preparation is arguably the most important factor contributing to the properties of the resultant material. When preparing nanocomposites, it is fundamental to ensure favorable interactions between the different constituents. In aqueous media preparation, the pH and ionic strength are two essential parameters that govern the behavior of charged nanoparticles and polyelectrolytes that must be controlled to avoid

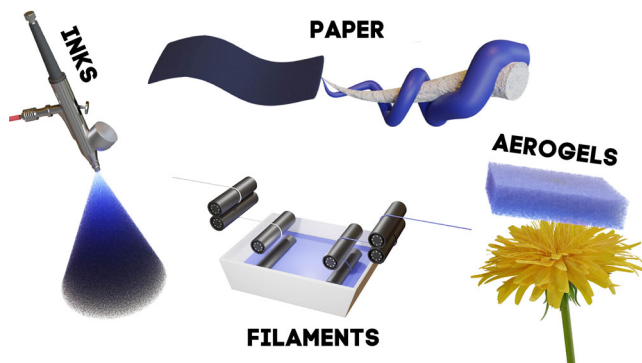


**Figure 5.** Illustration presenting the various forms of nanocellulose/PEDOT:PSS composites: inks, paper, filaments, and aerogels.

aggregation. The mixing and stresses applied to the materials to ensure a homogenous composite drastically influence the properties of a given material. Since cellulose and its derivatives are fiber based, the avenues to composite it with PEDOT:PSS are numerous. From the nanofiber level to large-scale sheets of cellulose, PEDOT:PSS can be combined with cellulose at any scale. Within this review, we have categorized the composites into four parts: electroactive inks, electroactive paper (both global and patterned), man-made electroactive filaments, and electroactive aerogels. Graphical illustrations of each composite can be seen in [Fig. 5](#).

#### 4.1. Electroactive inks

NCs as active components have gained popularity for printed electronic devices and the textile industry due to its rheological properties, hydrophilicity, and versatile surface chemistry. With the inherent hydroxyl groups on the surface, NCs are stable colloidal suspensions in water, and therefore make them a suitable candidate for use in direction ink printing (DIW). The anisotropic nature of NC hydrogels contributes to hydrodynamic alignment and disentanglement of the components when subjected to shear forces, and reorganization of the fibrous network decreases viscosity with increasing shear rate, known as shear-thinning effect. The combination of these NCs as a rheology modifier with conducting materials enhances shear-thinning flow behavior and colloidal stability of aqueous systems.<sup>[107]</sup> Good dispersions of NC and PEDOT:PSS nanocomposites can be prepared by simple blending in water to form conductive inks. To achieve this, the NC gel and/or PEDOT:PSS could be suspended in DI water to alter the interaction of nanofibrils.<sup>[25,26]</sup> Generally, these blended composites have been diluted and mixed or sonicated before various additives have been introduced. Glycerol has been shown to improve the mechanical flexibility and aids in avoiding delamination or cracking while DMSO has been used as a secondary dopant for the PEDOT:PSS component to increase the electrical conductivity of the composites. An eco-friendlier, secondary dopant substitute, EG, has been incorporated which has shown similar improvements to the electrical conductivity. Using the above as a base, different types of surface-modified CNF<sup>[83]</sup> in addition to other additives such as lignosulfonate<sup>[92]</sup> and ionic liquids<sup>[108]</sup> have been reported in the scientific literature. While there are many reports on the

blending of CNF and PEDOT:PSS, there is still room for improvements and the addition of other functionalities. One can imagine the adaption with different solvents, thermoelastic polymers or other conductive materials to promote stretchability, thermo-electric or triboelectric properties. However, it is important to ensure that the conductive ink can be adapted to large-scale production techniques such as paper making or printing technology. The benefit of adding NC into PEDOT:PSS will increase the viscosity, shear thinning behavior, surface wettability and compatibility. Since the viscosity of NC/PEDOT:PSS-based ink can be adjusted by water evaporation, this ink can be used for a variety of deposition techniques including drop casting, inkjet printing, screen printing, slot die coating, spray coating and 3D printing. Several works have been demonstrated that cellulose-PEDOT:PSS-based inks have been successfully employed by screen/stencil printing and spray coating.<sup>[27,109]</sup>

#### **4.2. Electroactive nanopapers**

NC and PEDOT have been widely used to prepare conductive or electronic nanopaper. These electronic nanopapers are classified into three categories which are electrically conductive ink on nanopaper, electrically conductive nanopaper (compositing of NC and conductive materials), and electronically conductive patterned nanopaper.

As opposed to paper, these nanopapers (paper-like substrates fabricated with NC) are not prepared from cellulosic pulp fibers and generally show submicron roughness. The preparation involves various types of cellulosic nanoparticles or polymers (native dissolved cellulose, CMC). Being densely packed, these films are generally used in applications where good mechanical properties (stiffness and strength) as well as high electronic conductivities are required.

A first compositing route consists in preparing cellulosic films (nanopaper as substrate) and post functionalizing them with PEDOT or a PEDOT derivative to form conductive ink on paper. Nanopapers are readily prepared from cellulosic solutions by solvent casting or precipitation in a non-solvent. Films can also be prepared using vacuum filtration of dispersions of CNCs and CNFs followed by vacuum drying or paper making machine.<sup>[25,26]</sup> Simple impregnation and drying procedures can be used to load cellulosic films with substantial amounts of PEDOT.<sup>[110]</sup> Several studies also reported the use of the Layer-by-Layer (LbL) to functionalize nanopapers with PEDOT.<sup>[111,112]</sup> This technique relies on the successive deposition of alternatively charged polyelectrolytes onto charged surfaces and can be used to deposit large amounts of active material. PEDOT:PSS carries a net negative charge due to an excess of counterion and can hence be used together with a polycation to functionalize surfaces through a LbL procedure. Functionalizing cellulosic films with large amount of PEDOT can also be achieved through polymerization of EDOT. When doing so, cellulosic films are impregnated with a solution of EDOT and the polymerization is triggered by the addition of an oxidant such as APS.<sup>[90]</sup> Different counterions such as TOS or PSS can be added to the reactive mixture, to increase the doping of the synthesized PEDOT. Polymerization of EDOT generally results in the deposition of thick layers of PEDOT nano- or microparticles, providing a good affinity between the conductive polymers and the substrate. With



advanced deposition techniques using printing, PEDOT:PSS inks can be directly printed on nanopaper substrate to produce electronically conductive ink.

A second type of compositing route, where PEDOT is incorporated prior to, or during, the film formation, has been extensively discussed in previous studies. Several of these studies demonstrate the electrochemical polymerization of EDOT in CNC dispersions, yielding the formation of composite films onto working electrodes.<sup>[113,114]</sup> Bearing sulfonate groups on their surface, CNCs act as a counterion to the synthesized PEDOT and provide the formed film with mechanical integrity. On the other hand, electronegative charge of sulfate groups on CNF allows positive charged EDOT monomers to interact with the CNF surface by electrostatic attraction force, and a CNF-PEDOT:PSS composite is formed after adding an APS oxidizing agent.<sup>[95]</sup> Recent studies have also investigated a one-pot preparation of cellulose and PEDOT:PSS composite films by casting aqueous dispersions of CNFs and PEDOT:PSS.<sup>[25,89,97,115]</sup> The authors demonstrated an increase in electronic conductivity when using DMSO in the dispersion, combined with a post-treatment of the films in EG. The prepared films showed outstanding mechanical properties, benefitting from the high stiffness and strength of CNFs, as well as record high combined electronic and ionic conductivities.

Thanks to high electrical conductivity, mechanical stability, biocompatibility, and biodegradability, electronically conductive nanopapers have been applied in disposable and flexible electronics for future energy harvesting and storage, bioelectronics, and sensor design, in particular for the development of green electronics.<sup>[29,83]</sup>

### **4.3. Man-made electroactive filaments**

Man-made filaments are characterized by having one dimension much larger than the other two and thus is being said to be one-dimensional. Filaments are used either as continuous or cut into stable fibers for further processing with applications ranging from clothing and upholstery to reinforcement in composites and even communication. They are produced from many different raw materials (polymers, metals, or minerals) by many different production processes, such as melt-, dry-, wet-, electro-spinning, etc.<sup>[116]</sup> It is predicted that filaments from bio-based sources in combination with conductive materials will play a more important role in our future society, especially in developing the growing e-textile industry. This includes applications such as wearable electronics for sports and daily life activities, and healthcare monitoring.<sup>[117]</sup>

Diving directly into recent scientific results, wet-spinning has recently been utilized to manufacture PEDOT:PSS filaments, which with an EG-treatment, resulted in a high conductivity of 3828 S/cm<sup>[118]</sup>, whereas its treatment with DMSO showed conductivity up to 3663 S/cm and tensile strength of 550 MPa<sup>[119]</sup>. The highly conductive and flexible fibers are suitable for use in smart textiles, flexible electrodes, and fast-response sensors and actuators.<sup>[120]</sup> Even though it is possible to produce pristine PEDOT:PSS filaments, it is of interest to combine the PEDOT:PSS with cellulose due to the biodegradability, low cost, high mechanical performance, and processability in water structuring of the cellulose but also due to the interactions mentioned above and other potential synergies when mixing a conductive polymer with an insulating one. Moreover, pristine PEDOT:PSS becomes brittle and has weak mechanical properties.

The combination of PEDOT:PSS and NC not only improves the mechanical properties but also allows the formation of conductive inks with a wide range of viscosity, enabling them for use in printed flexible electronics and energy storage devices, and many other applications.<sup>[8]</sup> Cellulose-based fiber materials and PEDOT:PSS have been successfully combined to form conductive filaments via different spinning processes (yarn spinning and dyeing) by blending or compositing, coating, and synthesis of PEDOT on cellulose yarns. Using a roll-to-roll dip coating technique, filaments made of PEDOT:PSS-DMSO/EG coated on cotton and silk yarns showed the conductivity of 14 and 70 S/cm, respectively.<sup>[121,122]</sup> However, electrical conductivities and mechanical properties of the filaments from cellulose fiber spun are relatively low and weak, respectively, resulting in a low degree of wash and wear resistance.<sup>[117]</sup> If the filament is supposed to be used in a clothing context, the filament composite materials needs to be washable, water resistance, and resistance to mechanical stress overtime.<sup>[123]</sup>

As an alternative to filaments manufactured from conventional cellulose fibers such as cotton or dissolved cellulose, spinning filaments from NC has been explored the last decade. An important benefit with using NC is that they are dispersible in water and avoid any hazardous solvents.<sup>[124,125]</sup> The mechanical performance of NC filaments depend on the control of alignment of the fibrils inside the filament and interactions in the nanofibrillar system.<sup>[116]</sup> Several works have used electro-spinning to form NC-PEDOT:PSS-based filaments. Latonen *et al.* prepared filaments from CNF-PEDOT:PSS-PEO composites via electro-spinning. They used poly(ethylene glycol) diglycidyl ether for chemical crosslinking to enable the stability of fibrous mats in water.<sup>[94]</sup> Another study used CNC-PVA-PEDOT:PSS composites with the addition of DMSO and EG (to reduce the electric field) to form filaments. By taking an advantage of electro-spinning, the electric field could induce alignment of the conductive fibrils, and, therefore, the mechanical strength of the filaments is expected to be higher than electronic paper. Furthermore, a water based wet spinning method, consisting of flow focusing equipment was developed to align and assemble CNF into continuous filaments.<sup>[126]</sup> A record in mechanical properties (tensile stiffness of 86 GPa and tensile strength of 1.6 GPa) has been reported based on the aforementioned method.<sup>[127]</sup>

The production of filaments created with NC and PEDOT:PSS is an opportunity for further understanding of the fundamentals of the interactions between the different materials due to the possibility for structure control. A question may be asked; will alignment of one material induce alignment in the other?

As previously mentioned PEDOT absorbs on the surface of NC to form a core-shell structure, therefore the CNF-PEDOT:PSS filaments will be given a core-shell structure as well, where the coated surface or shell represents a coherent entity with a dimension of the filament diameter. The framework of CNF-PEDOT:PSS filaments being absent of harmful solvents and its tunable properties, biodegradable properties, and material availability is believed to enable large scale production in the textile industrial.

#### **4.4. Electroactive aerogels**

CNFs, CNCs, and BC form aqueous gels at relatively low solid contents, depending on both the aspect ratio of the nanoparticles and their surface charge. These gels are

readily turned into high SSA, porous, and lightweight materials – also referred to as aerogels (containing more than 99% of air) – using freeze-drying or supercritical CO<sub>2</sub> drying.<sup>[128,129]</sup> The porous structure of these aerogel takes its origin from the formation of ice crystals during freezing. As water freezes, the cellulosic nanoparticles are progressively excluded from the growing ice crystals and densely compacted into mechanically strong lamellar structures. Due to the high affinity of cellulosic nanomaterials for water and the low degree of physical contact within the lamellae, these aerogels often disintegrate when soaked in water. In order to use the aerogels in applications that necessitate the presence of liquids, it is then important to maintain their structural integrity using either chemical or physical crosslinking.<sup>[130]</sup> As freeze-drying and supercritical CO<sub>2</sub> drying are highly time and energy consuming and batch-wise processes, researchers have recently demonstrated the preparation of cellulosic aerogels through successive freezing, solvent exchanging, and drying of CNF gels. For instance, CNF gel formulations containing high ionic strengths of CaCl<sub>2</sub> and NaCl allow the formation of strong lamellar structure upon freezing, which withstand ambient drying.<sup>[131]</sup>

CNF aerogels have been used in sensing and energy storage applications,<sup>[132]</sup> and various preparation and functionalization routes have been suggested.<sup>[132]</sup> They are particularly interesting substrates for these applications, as their high SSAs and open porous structures guarantee great contact with the electrolyte and ionic conductivity while also promoting fast ion adsorption/desorption from electrode through redox reaction. Additionally, a recent study also demonstrated the 3D printing of composite aerogels of CNFs and PEDOT:TOS, enabling applications where high-precision material shaping is needed, such as tissue engineering.<sup>[131]</sup> The 3D printing of NC gels and their processing into aerogels has been reported in other studies, which highlighted its potential in the fast preparation of highly-porous cellulosic substrates of intricate shapes<sup>[132,134]</sup>. The structure of NC aerogels has also been found to shrink and expand as environmental parameters such as temperature, pressure or humidity are changed, thus making them particularly interesting materials for sensing applications, when composited with electroactive materials such as PEDOT:PSS.<sup>[100]</sup> Han *et al.* reported the preparation of PEDOT:PSS, CNF, and glycidoxypropyl trimethoxysilane (GOPS) (an epoxy-like crosslinker) dispersions for use in sensors and solar steam generator after the dispersions were freeze-dried into aerogels.<sup>[91,135,136]</sup> The literature also has numerous examples of cellulosic aerogels post-functionalized with PEDOT, using either impregnation<sup>[134,137]</sup>, LbL<sup>[138]</sup> or *in situ* polymerization<sup>[131]</sup> approaches.

The various types of composites outlined within this section of the review highlight very different morphologies and structures. Generally, the structures are designed with certain applications in mind, tailoring the properties for the specific technology.

## 5. Fields of application

NC materials endow useful features such as high surface area, nanoporous structure, high mechanical strength, low coefficient of thermal expansion, water solubility, eco-friendliness, renewability, biocompatibility, and biodegradability character.<sup>[8,139]</sup>

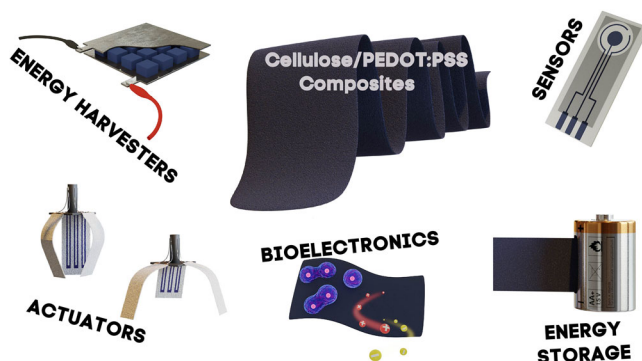


**Figure 6.** Cellulose/PEDOT:PSS composites incorporated into their main electroactive applications.

There exists extensive literature on the use of NCs in many fields of applications, ranging from paper industry and food packaging, membranes, filters, etc.<sup>[140]</sup> Using an insulating material such as cellulose or NC in a composite for use in opto-electronic applications may seem counter intuitive, however, the cellulose components are either incorporated as a supporting scaffolding for the PEDOT:PSS or as the substrate. Additionally, combining the porosity of cellulosic materials with electroactive PEDOT:PSS could be one avenue to allow access to the bulk PEDOT:PSS instead of being limited to the surface layer. The amounts of cellulose incorporated within the composite materials are also generally minimal to limit its insulating influence. Combining NC with PEDOT:PSS permits applications beyond those stated above by relying on their strengths of being light-weight, flexible, mechanical robust, and electronically and ionically conductive. The usefulness of a composite material is judged heavily by its performance in specific applications. Within this section we focus on electronics-related applications of CNF/PEDOT:PSS composites, specifically, energy storage and harvesting, sensors, actuators and bioelectronics devices (See Figure 6).

### **5.1. Energy storage**

PEDOT:PSS has been incorporated in supercapacitors since the discovery of its excellent mixed ionic-electronic conductivity, high specific capacitance (30 – 130 F/g) and its ability to act as both electrodes in a symmetric device.<sup>[141,142]</sup> The ability to easily transfer charge allows the porous, open structure of PEDOT films to provide an enormous effective surface area for charge transport. NC/PEDOT composites have been heavily researched in the areas of energy storage due to its stability, high capacitance and its alignment with the idea of sustainable, environmentally friendly energy storage solutions. The capacitance of NC/PEDOT composites has been investigated by using electrostatic models by comparing modeling and experimental methods.<sup>[143]</sup> Models such as these have and will continue to aid researchers in formulating NC/PEDOT composites that improve the overall performance of supercapacitors in addition to fabrication by printing techniques for large-scale production. Cellulose/PEDOT-based supercapacitors have been prepared by polymerization or blending as conductive ink and followed by casting or printing techniques to form paper supercapacitors, as listed in Table 1.

**Table 1.** Compiled supercapacitor compositions, characteristics, and performances using cellulose/PEDOT composites.

Materials	Solvents	Separator/ electrolytes	Methods/fabrication	Volumetric or specific energy	Volume metric or specific energy	Cycle stability (cycles/%)	References
Cellulose paper/PEDOT	n-Butanol	PVA/H <sub>2</sub> SO <sub>4</sub>	Polymerization/drying	1 mWh/cm <sup>3</sup>	50 mW/cm <sup>3</sup>	2500/90	[144]
Cellulose paper/ PEDOT:PSS/MWCNT	Ionic liquid	PVA/KOH	Polymerization/drying	4.86 Wh/kg	4.99 kW/kg	2000/95	[146]
Cellulose paper/PEDOT	—	Paper/PVA/H <sub>2</sub> SO <sub>4</sub>	Vapor phase polymerization	0.76 mWh/cm <sup>3</sup>	10 mW/cm <sup>3</sup>	1000/77	[145]
Cellulose/PEDOT:PSS	EG/glycerol	HEC/EMIM-ES	Conductive ink/ screen printing	2 Wh/kg	395 W/kg	10,000	[109]
Cladophora CNF/PEDOT	—	Paper/H <sub>2</sub> SO <sub>4</sub>	Polymerization/vacuum filtration/drying	3 Wh/kg	2.45 kW/kg	15,000/93	[142]
CNC/PEDOT:PSS	—	—	Electrochemical polymerization	11.44 Wh/kg	99.85 W/kg	1000/86	[114]
BC/PEDOT	—	PVA/H <sub>2</sub> SO <sub>4</sub>	Polymerization/drying			5000/93	[150]
CNF/PEDOT:PSS	DMSO/ glycerol	NFC-PSSH	Conductive ink/casting	1.016 Wh/kg	2040 W/kg		[117]
CNF/PEDOT: PSS-Alizarin	DMSO/ glycerol	Nafion membrane/ HEC-HClO <sub>4</sub>	Conductive ink/ casting	8.9 Wh/kg at 2 A/g	459 W/kg	1500	[151]
CNF/PEDOT:PSS	EG/glycerol	HEC/EMIM-ES	Conductive ink/ spray coating	0.57 Wh/kg at 1 A/g	22.3 kW/kg	2000/92	[27]

Synthetic strategies have been developed for the preparation of a flexible solid-state supercapacitor by in situ and vapor phase polymerizations of PEDOT into cellulose paper.<sup>[144,145]</sup> Another strategy by Zhou *et al.* introduced MWCNTs into cellulose/PEDOT:PSS to increase the specific energy and power and discharge cycle stability.<sup>[146]</sup> Recently, Brooke *et al.* reported cellulose/PEDOT:PSS solution-based inks to prepare paper supercapacitors using stencil/screen printings.<sup>[109]</sup> This study demonstrates a fast avenue for commercialization of low production cost if either the price for PEDOT:PSS can be lowered or if only a minimal amount of PEDOT:PSS is required for the composite to possess the appropriate functionality.

Another alternative that has been reported is to substitute the cellulose pulp fiber for NC. High SSA allows more sites for electrical double layers to form on the NC surface, and the porous structure provides more electroactive sites and ionic paths for diffusion, leading to high specific capacitance and life cycle. Jiao *et al.* developed the concept of nanopaper-based supercapacitors.<sup>[115]</sup> CNF/PEDOT:PSS nanopapers were used as both electrodes, and CNF-PSSH was used as the separator-electrolyte. NC allows the electrolyte to fill its porous structure network and give access for ionic species to transport easily to the bulk of electrode.<sup>[147]</sup> However, an increase of CNF-PSSH resistance dominates over the resistance of reduced PEDOT and poor interface adhesion between separator and electrode give high equivalent series resistance (ESR) (90 Ω), thus reducing the specific power of supercapacitor. Improving adhesion by using a gel electrolyte prepared by 0.1 M HClO<sub>4</sub>, hydroxyethyl cellulose (HEC), and the addition of alizarin as redox molecules from plant into CNF/PEDOT:PSS electrode could boost the performance of supercapacitor.<sup>[148]</sup>

To further demonstrate large area devices, Say *et al.* manufactured paper-based electrodes using CNF/PEDOT:PSS ink with spray coating and successfully implemented it onto flexible current collectors.<sup>[27]</sup> In this study, paper electrodes (7.6 μm) were deposited using simple air-brush technology onto flexible substrates with a smaller number of processing steps with controlled electrode thickness. Since both spray-coating and

screen printing allow paper electrodes to be fabricated directly on current collectors, solution-processed techniques have great potential to scale up improved devices both mechanically (adhesion) and also electrically (improved interfaces contribute to less resistive devices). The spray-coated paper supercapacitors demonstrate low ESR (0.22  $\Omega$ ), leading to  $10^4$  W/kg specific power and showed good stability under mechanical stress.

When these works are compared to other methods such as electrochemical and chemical polymerization<sup>[138,144,149]</sup>, solution-processed methods bring more functionality, large area coverage, and controlled mechanical form factors to device architecture. The selection of printing technology allows to fabricate pocket size and large-scale production of supercapacitors (roll-to-roll or sheet-by-sheet) for wearable and portable electronics, smart packaging or energy storage devices in general.

While the majority of work on energy storage devices has focused on supercapacitors, CNF/PEDOT:PSS composites have also been incorporated into fuel cell technology to potentially create clean, sustainable, and renewable energy by converting chemical energy to electricity energy.<sup>[29]</sup> Previously, PEDOT has been utilized as the electrocatalyst for the oxygen reduction reactions (ORR) with high efficiency, but lacks hierarchically structural integrity for electrodes in fuel cells.<sup>[151]</sup> From the cellulose point of view, many reports have shown NCs can be used as membranes for fuel cells due to their high thermomechanical and chemical stability, and tailorable surface chemistry.<sup>[29,33,152–154]</sup> The idea of combining these materials is tempting so to impart the electroactive PEDOT component with the mechanical integrity advantages of the NC. This idea has been shown in one publication which showed a successful fuel cell device using CNF/PEDOT:PSS composites as the electrodes. The CNF/PEDOT:PSS composite was created in a paper-making process and used as a gas diffusion electrode (cathode and gas diffusion layer) for polymer electrolyte membrane fuel cell (PEMFC) applications.<sup>[155]</sup> The fuel cell device was shown to produce a maximum power density of approximately  $50 \mu\text{W cm}^{-2}$ . The low power density is attributed to the low surface area and therefore the ability of the cellulose fiber for storing charge and the overall conductivity of the composite material. However, the gas diffusion electrode made from conductive CNF/PEDOT:PSS paper could act as electrocatalyst for supporting the electron transport to bipolar plates and as the electrode channel to assist the gas flow through its nanoporous gas diffusion layers. While only sparse reports have been published on the fuel cell technology aspects, the ability to create electrodes in paper making fashion will most likely lead to more research and development for the goal of large-scale energy storage.

## **5.2 Energy harvesting**

### **5.2.1. Thermoelectric generators**

Thermoelectric generators (TEG) and thermoelectricity, holds great interest in scientific and industrial communities due to low-cost energy resources including waste heat dissipated from industries and human body heat.<sup>[156]</sup> Organic thermoelectric materials are used for fabrication of miniaturized TEGs or flexible TEG devices that can harvest electricity from body heat to supply power to flexible, wearable, and implantable electronic

devices.<sup>[157]</sup> It has been reported that as-cast PEDOT:PSS films with its properties including flexibility, light weight, and low thermal conductivity, ranging from 0.1 to 0.5 W/mK, has potential within organic TEG.<sup>[75]</sup> Another advantage is that the output power from PEDOT:PSS can be harvested at very low-temperature gradients between the hot and cold side.<sup>[158]</sup> However, its intrinsically thermoelectric (TE) properties (electrical conductivity and seebeck coefficient) are relatively low, and therefore improvements are required to meet the applications. Enhancement of the power efficiency can be done in two ways. The first route is achieved by doping and de-doping, post-treatment, and alignment using acid, organic solvents, and ionic liquid treatment<sup>[157]</sup>. Whereas the second route can be performed by blending or compositing with other polymer components<sup>[75]</sup>. Fan *et al.* used H<sub>2</sub>SO<sub>4</sub> and NaOH to treat neat PEDOT:PSS. The PEDOT:PSS film had conductivity of 2170 S/cm, seebeck coefficient of 39.2  $\mu\text{V/K}$ , and power output of 334  $\mu\text{W/K}^2\text{m}$ .<sup>[159]</sup> The authors later reported a record breaking figure of merit (ZT) value of 0.75 and high power factor of 754  $\mu\text{W/K}^2\text{m}$  by treating PEDOT:PSS with 1-ethyl-3-methylimidazolium dicyanamide (EMIM-DCA).<sup>[160]</sup> The post-treatment facilitates effective depletion and phase segregation of the PSS chains and induces conformational change in the PEDOT chains from benzoid to quinoid structures, which allows for an improved charge transport pathway.<sup>[159]</sup>

Darabi *et al.* successfully fabricated 40 out-of-plane thermocouples of CNF/PEDOT:PSS yarn as the p-type and silver embroidery yarn as the n-type using a sewing machine. With Seebeck coefficients of 14.6  $\mu\text{V/K}$  p-type and of 0.3  $\mu\text{V/K}$  n-type at 37 °C, the maximum power output reached 210 nW, and this value can be further increased by increasing the number of thermocouples.<sup>[117]</sup> The result shows a promising application for e-textiles using a conventional sewing machine. Furthermore, aerogel CNF-PEDOT:PSS can be used for thermoelectric sensors, which will be discussed in the sensor application section.<sup>[137]</sup> In one aspect, the combination of PEDOT:PSS with CNF-PSSNa (high ionic conductivity of 9 mS/cm and seebeck coefficient of 8.4 mV/K), the device can function as an ionic thermoelectric supercapacitor and a gate organic transistor.<sup>[161,162]</sup>

One of the important properties of a thermoelectric material is its thermal conductivity which should be minimized in order to sustain a temperature gradient. Brill *et al.* studied the thermal diffusivity, which is directly proportional to the thermal conductivity, of CNF/PEDOT:PSS nanopapers using a novel photothermal technique.<sup>[163]</sup> In their work, they investigated both the in-plane and transverse (through-plane) diffusivity of the nanopaper and could conclude that the in-plane diffusivity was 2–3 times larger than the transverse diffusivity (0.7 mm<sup>2</sup>/s compared to 0.25–0.4 mm<sup>2</sup>/s). Similar anisotropic transport properties have been observed for the electrical conductivity for the same nanopaper composite and is believed to be the result of the anisotropic structure of the material resulting from polymers and fibers having a preferential orientation along the plane during film formation.<sup>[98]</sup> Since a small thermal diffusivity is desired in TEG, this suggests that when using CNF/PEDOT:PSS nanopapers, the transverse direction is favorable to use in the design of the devices. Such device structures are also more easily realized due to the mechanical strength of the nanopapers which enables them to be self-supporting. Brill *et al.* further concluded that the transverse thermal diffusivity was inversely proportional to the thickness of the samples. This result was not

expected as the diameter and length of the fibrils are much smaller compared to even the thinnest sample. Instead, the authors claim that differences in the film formation and water content might give rise to the thickness dependence. The results therefore show that thicker (and therefore more mechanically stable) films are more suitable for use in thermoelectric power generation. However, the smaller electrical conductivity in the transverse direction of the paper might be an issue. While the thermal diffusion should be kept small, it is desired to have as small as possible electrical resistance in order to maximize thermoelectric power output. The smaller conductivity of PEDOT:PSS in the transverse direction compared to the in-plane direction is well documented and can differ by 2–4 orders of magnitude.<sup>[164]</sup> However, Wang *et al.* demonstrated that for CNF/PEDOT:PSS nanopapers, this conductivity ratio could be smaller than one order of magnitude.<sup>[98]</sup>

### 5.2.2. Photovoltaics

Photovoltaic cells, or solar cells, are one of the most commonly used energy harvesting devices. In 2018, photovoltaics accounted for ~6% of the global production of renewable energy according to the International Energy Agency<sup>[165]</sup>, and this number is expected to continue to grow rapidly in the coming years. Although this technology is often considered to be “green,” there are many environmental, health and safety issues related to the production and disposal of solar cells. Composites of NC/PEDOT:PSS not only address some of these environmental issues but can also provide a flexible substrate for photovoltaics.

Gao *et al.* utilized thin and transparent NC films as a substrate to produce flexible perovskite solar cells.<sup>[166]</sup> The substrate was made conductive by coating the NC film with doped PEDOT:PSS. An additional PEDOT:PSS layer (with a different composition) was added on top of the conduction layer as a whole-injection layer. Since PEDOT:PSS is highly transparent, light could pass through both the substrate and conductive layers with little absorption. The authors claim that the devices are more environmentally friendly since they do not use petroleum-based transparent substrates, and that the solar cells can be disposed of by combustion.

Besides the traditional inorganic solar cells, new device concepts have recently emerged that could potentially be more sustainable. One such device is the biohybrid photovoltaic cell which mimics the photosynthesis of plants for generating energy. In their work, Méhes *et al.* demonstrated how CNF/PEDOT:PSS composites could be used as one of the charge collecting working electrodes in such devices.<sup>[167]</sup> This novel type of solar cell uses visible light to photoexcite certain molecules derived from plants which, together with a redox mediator, can drive an electrical current. However, they addressed that the solar cells power could be further enhanced by irradiating the CNF/PEDOT:PSS electrode with IR-radiation. The combination of the high capacitance of the electrode and the good IR-absorption of PEDOT:PSS resulted in a 6-fold enhancement of power output. The authors attribute the improvement to an ionic thermoelectric effect, together with the redox-mechanism. This type of device not only uses more bio-based components compared to traditional solar cells, but also utilizes a larger part of the solar spectra by using the IR-part. An important step forward in more efficient, sustainable energy harvesting.



### 5.3. Sensors

#### 5.3.1. Paper sensors

Paper-based sensors are an attractive technology due to the low cost and the potential of biodegradable, one-time, on-site use sensors.<sup>[168]</sup> Cellulose/PEDOT:PSS composites for the application of sensors can provide both a flexible substrate or framework in addition to the active sensing component. If paper-making processes can be adapted to these composites, one can imagine paper machines fabricating thousands of sensors an hour which, after their use, can be disposed of responsibly and sustainably.

Sensors based on cellulose/PEDOT:PSS composites have been created in a variety of ways utilizing both cellulose as the substrate with PEDOT:PSS deposited on top as well as PEDOT:PSS integrated into cellulose such as aerogels. The simplest avenue to create cellulose/PEDOT:PSS sensors is by drop casting onto cellulose paper. While simple in its manner, researchers have been able to exploit this method to create pressure sensors. Paul *et al.* used this technique (graphene oxide was also included with the PEDOT:PSS) with graphite paper and tissue paper in a symmetric device to measure pressure. When pressure was applied, the paper composite compressed and the resistance was lowered, a good example of a simple manufacturing technique that can be used to create a simple sensor.<sup>[169]</sup>

Moving from the simplest techniques forward, researchers have produced paper sensors based on cellulose and PEDOT:PSS by using common desktop inkjet printers with the usual colored pigment replaced with functional inks. Both humidity and temperature sensors have been fabricated using the inexpensive printers. The humidity sensor was achieved by Morais *et al.* by combining polyaniline and PEDOT:PSS in an ink and printing on standard bond paper. Although the humidity sensor relied heavily on polyaniline, the PEDOT:PSS electrodes were an important aspect of the device. The sensor showed a good linear resistance response to humidity; however, the range of humidity was from 16% to 98%.<sup>[170]</sup> It is unclear how sensitive the device is when only minimal changes in humidity occur. Perhaps with a change in sensor design such sensitivities could be achieved.

The temperature sensor was developed by utilizing thermoelectric technology where PEDOT:PSS acted as the p-junction and carbon nanotubes (with conductivity boosted by silver nanoparticles) were used as the n-junction.<sup>[107]</sup> After three printed layers, homogenous films were achieved in a simple device design. The temperature sensor showed good linear relationship within the temperature range of room temperature to 150 °C. Again, the range is large with some variation on the linear scale suggesting that this sensor may be inadequate with minimal variation in temperature.

While these sensors use standard and inexpensive printers to manufacture functional devices, if highly sensitive data is required, it would appear, they would not be appropriate unless changes to the designs or materials are optimized. However, when large humidity and temperatures are required to be tracked or sensed, these devices would be perfect for cheap and easy solutions. It could be argued that the measuring of the sensors above requires complex equipment, but it can be envisioned that once established, the sensors can be incorporated in (possibly printed) electronics with simple construction for accurate read outs making them accessible, low-cost and reliable.

Producing paper sensors on a common printer is a big step forward in paper-based sensors as it has the potential to be produced by anyone, anywhere (provided they can be supplied with the correct ink) instead of technology that requires specific and expensive equipment. An important aspect of the technology is, for example, essential bioelectronic sensing in isolated areas is required.

More complicated inkjet printed structures, requiring more advanced inkjet printers (Dimatix) were performed by Ruecha *et al.* to allow potentiometric sensing devices.<sup>[171]</sup> Within layer depositions including wax, silver (nanoparticle ink), iron chloride, potassium chloride and a graphene/PEDOT:PSS ink, the more extensive printing allowed 90 potentiometric sensing devices to be printed on an A4-sized paper substrate. The devices showed good sensitivity toward  $\text{Na}^+$  and  $\text{K}^+$  ions with a negligible sensitivity to other common ions such as  $\text{Mg}^{2+}$  and  $\text{Ca}^{2+}$ . Good sensing ability was also shown to the ions in human urine compared to conventional ion sensing technology. The comparison with other, more established sensing technology, is a great addition to this report and shows that the paper sensor technology is more than just a publication and that it has the potential to compete with other technology while bringing its own advantages. The technology now needs to be evaluated for its cost-effectiveness and whether the process can be optimized and upscaled to achieve large scale, sustainable, one-time use paper sensors.

### 5.3.2. Aerogel sensors

Within this review article, we have discussed aerogels and their large surface area structures. It comes as no surprise that the large surface area structures have been utilized for sensing applications. Due to the large porosity and low density of the NC/PEDOT:PSS aerogels, pressure sensors are simple to manufacture with sensing achieved *via* resistance measurements. When the aerogel is compressed, more electrical connections are created, and the resistance is reduced. NC/PEDOT:PSS aerogels have also shown great properties in regard to their thermoelectric ability due to their low thermal conductivity. Therefore, they can drastically outperform their solid counterparts with the same amount of material in thermoelectric sensing. Finally, aerogels, since they are freeze-dried in their fabrication, their uptake of water in humid environments is well known. Therefore, the ability to create humidity sensors from aerogels was only a matter of time. Due to these attributes, CNF/PEDOT:PSS aerogels for pressure, temperature, and humidity sensors have been reported.

Khan *et al.* first fabricated pressure and temperature sensors using CNF/PEDOT:PSS aerogels with the added ingredient of GOPS for elasticity purposes.<sup>[172]</sup> Han *et al.* then optimized the aerogels with a DMSO treatment.<sup>[91]</sup> The commonly used DMSO molecule acted as a secondary dopant to the PEDOT:PSS and increased the conductivity of the aerogel composite over two orders of magnitude from 0.0001 to 0.03 S/cm. As a result, the pressure sensitivity was increased. Han and his coworkers went further with a new design to increase the sensing to humidity.<sup>[135]</sup> Using electronic and ionic seebeck effects, the authors were able to measure temperature and humidity (in addition to pressure) independently of each with only minimal crosstalk.

Other research groups have achieved CNF/PEDOT:PSS aerogels as pressure sensors and stain sensors using different silane materials. GOPS (as well as polyethyleneimide)

was used to create crosslinks within the CNF/PEDOT:PSS and form Si-O-C bonds by Cheng *et al.* for pressure sensing.<sup>[137]</sup> The functional aerogels exhibited a drop in resistance with the onset of pressure but when compressed heavily did recover 100% of their original shape. Possibly as a result, their resistance vs. pressure results were not linear. There was also significant change in resistance between the compression and relaxation cycles the authors attribute to the changes in contacts between the outer electrodes.

As an alternative to using GOPS, Zhou and coworkers used poly(dimethylsiloxane) (PDMS), an alternative elastic polymer.<sup>[100]</sup> After optimization of the components, a sensitive strain sensor with high linearity from 0% to 95% strain was realized. Their PDMS-infused NC/PEDOT:PSS aerogel was compared to an aerogel without NC which showed 7 times better performance.

Freeze drying is an established technology on the large scale (instant coffee), so one can imagine producing NC/PEDOT:PSS aerogels in large volumes for commercial sensing applications.

#### 5.4. Actuators

With all the advantages of paper, it is no surprise that actuators have gained attention of researchers and their NC/PEDOT:PSS composites. With paper's advantages of low cost, light-weight, and large volumes of productions, it is already a desirable material but for actuator applications, paper's large deformation, dryness, and porosity make it essentially ideal.<sup>[173]</sup> Using the conductive polymer, PEDOT:PSS, in combination with cellulose for the application of actuation permits the PEDOT:PSS's electrochemical stability with low operating voltages to be added to the benefits. Actuation has been achieved using cellulose/PEDOT:PSS composites by depositing PEDOT:PSS onto cellulose paper<sup>[87,174–176]</sup>, NC<sup>[108,177,178]</sup> and using cellulose aerogels with PEDOT:PSS electrodes.<sup>[88]</sup> While this section aims to highlight previous reports on cellulose/PEDOT:PSS composites, the fundamentals and mechanism are not discussed. A recent review that focuses on PEDOT:PSS actuators, their structures, mechanisms, and fundamentals can be found here.<sup>[179]</sup>

By far the most common type of actuator utilizing PEDOT:PSS and cellulose is depositing PEDOT:PSS onto paper due to the simplistic design. In a few steps a working actuator can be manufactured. Hamedi *et al.* achieved cellulose/PEDOT:PSS actuators by printing wax to restrict the soaking of PEDOT:PSS into the paper.<sup>[174]</sup> With their designs, they highlighted the effect of humidity on the actuation while reporting a simple, cost-effective technique that can be easily integrated into printed electronics.

More advanced procedures of coating PEDOT:PSS onto paper have involved bar coating<sup>[87]</sup> and dip-coating.<sup>[175]</sup> Jain *et al.* produced a composite of cellulose/PEDOT:PSS using bar coating to produce butterfly-like motion. The impressive design allows intense bending with the onset of electrical stimulus.<sup>[87]</sup> Going one step further, Mahadeva *et al.* included polyelectrolytes within a cellulose/PEDOT:PSS composite to improve the actuators by reducing the energy consumption while enhancing the durability.<sup>[175]</sup> Others have improved their paper actuators by using additional conductive materials in their composites. Nan *et al.* used graphene nanopowders within their cellulose/PEDOT:PSS actuators which improved the actuation-specific capacitance, young's

modulus, response time and deformation.<sup>[176]</sup> This further compositing could be an avenue to improve and enhance the complicated functions and mechanisms of actuators in order to bring them to a competitive level on the commercial scale.

The above examples of PEDOT:PSS deposited onto paper as actuators are impressive and are an important starting point. Since commercial PEDOT:PSS inks are available for screen and inkjet printing, unique patterned structures can be achieved and used as actuators. It would seem reasonable to suggest that reports and even products are soon to be realized.

Turning to nanocomposites, composites of NC and PEDOT:PSS have also been investigated for their use as actuators. BC with carboxylic group modification has been composited with PEDOT:PSS and ionic liquid.<sup>[177]</sup> The modification of BC were shown to increase the ionic conductivity and ionic capacity of the material in addition to an eight times increase in deformation. Other researchers have also incorporated ionic liquids with CNF/PEDOT:PSS composites.<sup>[108]</sup> One such study showed that the CNF/PEDOT:PSS composite actually outperformed a similar device substituting carbon nanotubes with CNF. This result shows that the CNF has a large contributing factor to the function of the actuators and not simply a platform. Further compositing within the material with ionic liquids and ruthenium oxide has been reported and shown to also enhance the nanopaper actuators.<sup>[178]</sup>

It is clear from the reports within this section that ionic liquids are one material that is proven to enhance the cellulose/PEDOT:PSS actuators. One avenue to increase the absorbability of ionic liquid in the cellulose materials is to use aerogels. Kim *et al.* successfully created BC/PEDOT:PSS aerogels through freeze-drying techniques in order to create extremely light-weight actuators.<sup>[88]</sup> The aerogel actuators were shown to deform by 1.5 mm using 1 V. With the extreme lightness of aerogels, researchers will most likely apply similar techniques to improve aerogel actuator properties and performances as those of paper actuators. Therefore, more complex composites could be seen in the near future.

Some challenges that are present within all these reported actuators and a common issue faced with all paper electronics is the effect humidity has on paper. Paper and aerogels will absorb water from the environment which may limit their application in humid situations. Regardless of this challenge, these reports on cellulose/PEDOT:PSS composite actuators give the impression that artificial muscles and soft robotics could be seen using similar composites in the years to come.

### **5.5. Bioelectronics**

Cellulose/PEDOT:PSS composites may not yet have any direct applications in the human body. However, on-skin applications and wearable devices require the interface between materials and cells to be investigated. Paper biosensors attached to the body and wound dressings with electrochemical release of antibacterial drugs are excellent examples of future bioelectronic applications that can be foreseen for cellulose/PEDOT:PSS composites. Therefore, researchers have investigated the biocompatibility and cell growth on cellulose/PEDOT:PSS composites. It comes as little surprise that BC has dominated this application since it is the purest version of natural cellulose. The

basic tests for a material and its application into the bioelectronics field are the growth and survival of cells within or on the material. Previous studies reported that, individually, BC<sup>[180]</sup> and PEDOT:PSS<sup>[30]</sup> exhibit good biocompatibility and have shown minimal cell death observed through staining tests. As expected, the composites of cellulose and PEDOT:PSS have shown similar results. Most studies showed that the cell growth was similar if not better than pure BC. The consensus for the improvement is thought due to the rougher surface of the composites. Two studies investigated the PEDOT:PSS content in the composites and the effect each component had on the cells. As reported previously, PEDOT is a biocompatible material but the monomer, EDOT is toxic to cells. The danger in using any composite with PEDOT incorporated is that there may be unreacted EDOT monomers in the material. Chen *et al.* showed that with the increase in PEDOT in a NC/PEDOT (no PSS) composite, the cell percentage was lowered, leading to an optimized composite for biocompatibility that was relatively low in PEDOT content.<sup>[181]</sup> The authors hypothesized that it may indeed be due to unreacted EDOT in their composites. In another study within the same research group, the PSS content in the composite was investigated.<sup>[182]</sup> Interestingly, the trend was similar. With the increase in PSS, the cell percentage was decreased. This throws some doubt on the EDOT monomer presence in the previously mentioned study. Further investigation into the cell percentage decrease is needed which may be due to other factors than simply unreacted monomer species.

Researchers have gone further by using the BC/PEDOT:PSS composites as electrodes and stimulating the cells electrically. In order to be used as an electroactive material within biological systems, first the composites must be able to be electrically stimulated while only minimally effecting the cells. These investigations may be important for drug delivery applications and sensing within the sensitive biological environments. Chen *et al.* investigated the electrical stimulation of a BC/PEDOT:PSS/graphene oxide composite in the presence of P12 neural cells.<sup>[183]</sup> In their cytotoxicity studies prior to electrical stimulation, the percentage of live cells were similar to that of their standard tissue culture plate control. With the onset of electrical stimulation, no cell death was observed, neurite length and alignment with electric field was increased. Others showed that the electrical stimulation of the cells was more successful than other materials such as ITO and Au.<sup>[110,181]</sup> Further comparisons of materials including Au on BC, PEDOT:PSS on glass and PEDOT:PSS on BC was put forth by Inacio *et al.* for bioelectronic sensing applications.<sup>[110]</sup> Within this report, the signal-to-noise ratio when detecting signals in non-electrogenic cell populations was investigated by each type of electrode. Their results showed that PEDOT:PSS on BC was vastly superior to the other two. The authors state that these materials could have applications in neuron communications or in cancer research.

In addition to sensing, BC/PEDOT:PSS composites have been used as release vessels that could find applications in micro-dose and extensive period drug delivery systems. Initial investigations into BC/PEDOT:PSS as a component release vessel have shown promising results. Potential for on-skin applications with the releasing of metal ions was reported by Fu *et al.*<sup>[184]</sup> Copper and zinc ions, with their anti-bacterial and cell proliferation properties, were trialed as release components in both PPy and PEDOT:PSS/cellulose composites. Their results showed that the cellulose/PEDOT:PSS

composites far outperformed the PPy counterpart in terms of amount of ions released. The amount of cell proliferation was also considerably higher for the PEDOT:PSS composites justifying its use over other conductive polymers for this application.

In another study, the model drug, diclofenac sodium, was reported to be loaded and released from fibers of the cellulose/PEDOT:PSS composite.<sup>[185]</sup> The authors hypothesized that drug molecules could be delivered by the electrically responsive BC/PEDOT:PSS composites. Their results suggested that the composite material held the drug molecules appropriately with a linear release curve showing control release. The authors suggest that the fiber-based composite does not experience a burst release of drug commonly experienced by microparticle composites.

With bioelectronic applications of cellulose/PEDOT:PSS composites showing promising results in the areas of cell growth and drug loading/release, one can imagine a paper making process of cellulose/PEDOT:PSS material ready for use as bandages or other on skin applications. As the research progresses, we may see these materials loaded with antibacterial molecules to aid in preventing infections or even provide treatment.

## 6. Conclusion and perspectives

Within this review cellulose derivatives and PEDOT:PSS composites have been discussed in-depth. We have discussed the importance of fundamental research on the composites to understand the interactions and how the materials can be improved and what applications they may be most suited to. The procedures that have been used to combine cellulose derivatives and PEDOT:PSS have been outlined which have shown very different morphologies and structures that have been tailored to specific applications. These applications, with a focus on electrical/electronic devices, have been reviewed and the performance of the composites discussed. The applications of cellulose/PEDOT:PSS composites presented within this review are impressive milestones for the material and give hope for the future where similar materials may provide solutions to serious problems that plague society. However, for the serious uptake of these materials PEDOT:PSS must be manufactured in larger batch quantities in order to lower the price to increase industrial interest and the eventual large scale roll out of cellulose/PEDOT:PSS composites for these applications. With electroactive paper being one type of cellulose/PEDOT:PSS composite, it seems reasonable to suggest the future will bring roll-to-roll manufactured electroactive paper that uses existing paper making technology. A further step in the technology without the need to establish an expensive production line.

The overall picture of cellulose/PEDOT:PSS composites and the research conducted on them is bright. Many researchers have achieved impressive results within the laboratory and further research is being conducted to scale up these materials to combat real world problems. With a push for digitalization with sustainability, cellulose/PEDOT:PSS composites are destined to be a part of our future.

## Acknowledgments

The authors would like to acknowledge funding from Vinnova for the Digital Cellulose Competence Center (DCC), Diary number 2016–05193, the Swedish Foundation for Strategic Research (GMT14-0058) and the Wallenberg Wood Science Centre.

## Conflicts of interest

The authors declare no conflicts of interest.

## Funding

The work was supported by Vinnova for the Digital Cellulose Competence Center (DCC), Diary number 2016–05193, the Swedish Foundation for Strategic Research (GMT14-0058), the Wallenberg Wood Science Centre, Tresearch.se.

## ORCID

Robert Brooke  <http://orcid.org/0000-0001-8485-6209>

Makara Lay  <http://orcid.org/0000-0003-3227-085X>

Jesper Edberg  <http://orcid.org/0000-0002-2904-7238>

## References

1. Lupo, D.; Clemens, W.; Breitung, S.; Hecker, K. OE-A Roadmap for Organic and Printed Electronics. In *Applications of Organic and Printed Electronics. Integrated Circuits and Systems*; Cantatore, E., Ed. Boston: Springer: New York, NY, **2013**; pp 1–26.
2. Kim, J.; Kumar, R.; Bandodkar, A. J.; Wang, J. Advanced Materials for Printed Wearable Electrochemical Devices: A Review. *Adv. Electron. Mater.* **2017**, *3*, 1600260–1600215. DOI: [10.1002/aelm.201600260](https://doi.org/10.1002/aelm.201600260).
3. O' Mahony, C.; Haq, E.U.; Silien, C.; Tofail, S.A.M. Rheological Issues in Carbon-Based Inks for Additive Manufacturing. *Micromachines* **2019**, *10*, 1–24. DOI: [10.3390/mi10020099](https://doi.org/10.3390/mi10020099).
4. Saidina, D. S.; Eawwiboonthanakit, N.; Mariatti, M.; Fontana, S.; Hérold, C. Recent Development of Graphene-Based Ink and Other Conductive Material-Based Inks for Flexible Electronics. *J. Elec. Mater.* **2019**, *48*, 3428–3450. DOI: [10.1007/s11664-019-07183-w](https://doi.org/10.1007/s11664-019-07183-w).
5. Dai, L.; Cheng, T.; Duan, C.; Zhao, W.; Zhang, W.; Zou, X.; Aspler, J.; Ni, Y. 3D Printing Using Plant-Derived Cellulose and Its Derivatives: A Review. *Carbohydr. Polym.* **2019**, *203*, 71–86. DOI: [10.1016/j.carbpol.2018.09.027](https://doi.org/10.1016/j.carbpol.2018.09.027).
6. Ventura, C.; Pinto, F.; Lourenço, A. F.; Ferreira, P. J. T.; Louro, H.; Silva, M. J. On the Toxicity of Cellulose Nanocrystals and Nanofibrils in Animal and Cellular Models. *Cellulose* **2020**, *27*, 5509–5544. DOI: [10.1007/s10570-020-03176-9](https://doi.org/10.1007/s10570-020-03176-9).
7. Sabo, R.; Yermakov, A.; Law, C. T.; Elhajjar, R. Nanocellulose-Enabled Electronics, Energy Harvesting Devices, Smart Materials and Sensors: A Review. *J. Renew. Mater.* **2016**, *4*, 297–312. DOI: [10.7569/JRM.2016.6341](https://doi.org/10.7569/JRM.2016.6341).
8. Sharma, A.; Thakur, M.; Bhattacharya, M.; Mandal, T.; Goswami, S. Commercial Application of Cellulose Nano-Composites – a Review. *Biotechnol Rep (Amst)* **2019**, *21*, e00316–e00316. DOI: [10.1016/j.btre.2019.e00316](https://doi.org/10.1016/j.btre.2019.e00316).
9. Ooi, Y.; Hanasaki, I.; Mizumura, D.; Matsuda, Y. Suppressing the Coffee-Ring Effect of Colloidal Droplets by Dispersed Cellulose Nanofibers. *Sci. Technol. Adv. Mater.* **2017**, *18*, 316–324. DOI: [10.1080/14686996.2017.1314776](https://doi.org/10.1080/14686996.2017.1314776).
10. Nordenström, M.; Fall, A.; Nyström, G.; Wågberg, L. Formation of Colloidal Nanocellulose Glasses and Gels. *Langmuir* **2017**, *33*, 9772–9780. DOI: [10.1021/acs.langmuir.7b01832](https://doi.org/10.1021/acs.langmuir.7b01832).
11. Fall, A. B.; Lindström, S. B.; Sundman, O.; Ödberg, L.; Wågberg, L. Colloidal Stability of Aqueous Nanofibrillated Cellulose Dispersions. *Langmuir* **2011**, *27*, 11332–11338. DOI: [10.1021/la201947x](https://doi.org/10.1021/la201947x).

12. Klar, V.; Pere, J.; Turpeinen, T.; Kärki, P.; Orelma, H.; Kuosmanen, P. Shape Fidelity and Structure of 3D Printed High Consistency Nanocellulose. *Sci. Rep.* **2019**, *9*, 1–10. DOI: [10.1038/s41598-019-40469-x](https://doi.org/10.1038/s41598-019-40469-x).
13. Hoeng, F.; Bras, J.; Gicquel, E.; Krosnicki, G.; Denneulin, A. Inkjet Printing of Nanocellulose-Silver Ink onto Nanocellulose Coated Cardboard. *RSC Adv.* **2017**, *7*, 15372–15381. DOI: [10.1039/C6RA23667G](https://doi.org/10.1039/C6RA23667G).
14. Jiao, S.; Zhou, A.; Wu, M.; Hu, H. Kirigami Patterning of MXene/Bacterial Cellulose Composite Paper for All-Solid-State Stretchable Micro-Supercapacitor Arrays. *Adv Sci (Weinh)* **2019**, *6*, 1900529. DOI: [10.1002/advs.201900529](https://doi.org/10.1002/advs.201900529).
15. Hamed, M. M.; Hajian, A.; Fall, A. B.; Håkansson, K.; Salajkova, M.; Lundell, F.; Wågberg, L.; Berglund, L. A. Highly Conducting, Strong Nanocomposites Based on Nanocellulose-Assisted Aqueous Dispersions of Single-Wall Carbon Nanotubes. *ACS Nano* **2014**, *8*, 2467–2476. DOI: [10.1021/nn4060368](https://doi.org/10.1021/nn4060368).
16. Lay, M.; Méndez, J. A.; Pèlach, M. À.; Bun, K. N.; Vilaseca, F. Combined Effect of Carbon Nanotubes and Polypyrrole on the Electrical Properties of Cellulose-Nanopaper. *Cellulose* **2016**, *23*, 3925–3937. DOI: [10.1007/s10570-016-1060-5](https://doi.org/10.1007/s10570-016-1060-5).
17. Bacakova, L.; Pajorova, J.; Tomkova, M.; Matejka, R.; Broz, A.; Stepanovska, J.; Prazak, S.; Skogberg, A.; Siljander, S.; Kallio, P. Applications of Nanocellulose/Nanocarbon Composites: Focus on Biotechnology and Medicine. *Nanomaterials* **2020**, *10*, 196–134. DOI: [10.3390/nano10020196](https://doi.org/10.3390/nano10020196).
18. Dias, O. A. T.; Konar, S.; Leão, A. L.; Yang, W.; Tjong, J.; Sain, M. Current State of Applications of Nanocellulose in Flexible Energy and Electronic Devices. *Front. Chem.* **2020**, *8*, 420. DOI: [10.3389/fchem.2020.00420](https://doi.org/10.3389/fchem.2020.00420).
19. Nyström, G.; Mihranyan, A.; Razaq, A.; Lindström, T.; Nyholm, L.; Strømme, M. A Nanocellulose Polypyrrole Composite Based on Microfibrillated Cellulose from Wood. *J. Phys. Chem. B* **2010**, *114*, 4178–4182. DOI: [10.1021/jp911272m](https://doi.org/10.1021/jp911272m).
20. Muller, D.; Rambo, C. R.; Porto, L. M.; Schreiner, W. H.; Barra, G. M. O. Structure and Properties of Polypyrrole/Bacterial Cellulose Nanocomposites. *Carbohydr. Polym.* **2013**, *94*, 655–662. DOI: [10.1016/j.carbpol.2013.01.041](https://doi.org/10.1016/j.carbpol.2013.01.041).
21. Hu, W.; Chen, S.; Yang, Z.; Liu, L.; Wang, H. Flexible Electrically Conductive Nanocomposite Membrane Based on Bacterial Cellulose and Polyaniline. *J. Phys. Chem. B* **2011**, *115*, 8453–8457. DOI: [10.1021/jp204422v](https://doi.org/10.1021/jp204422v).
22. Gopakumar, D. A.; Pai, A. R.; Pottathara, Y. B.; Pasquini, D.; Carlos de Moraes, L.; Luke, M.; Kalarikkal, N.; Grohens, Y.; Thomas, S. Cellulose Nanofiber-Based Polyaniline Flexible Papers as Sustainable Microwave Absorbers in the X-Band. *ACS Appl. Mater. Interfaces* **2018**, *10*, 20032–20043. DOI: [10.1021/acsami.8b04549](https://doi.org/10.1021/acsami.8b04549).
23. Mantione, D.; del Agua, I.; Sanchez-Sanchez, A.; Mecerreyes, D. Poly(3,4-Ethylenedioxythiophene) (PEDOT) Derivatives: Innovative Conductive Polymers for Bioelectronics. *Polymers* **2017**, *9*, 354. DOI: [10.3390/polym9080354](https://doi.org/10.3390/polym9080354).
24. Montibon, E.; Järnström, L.; Lestelius, M. Characterization of Poly(3,4-Ethylenedioxythiophene)/Poly(Styrene Sulfonate) (PEDOT:PSS) Adsorption on Cellulosic Materials. *Cellulose* **2009**, *16*, 807–815. DOI: [10.1007/s10570-009-9303-3](https://doi.org/10.1007/s10570-009-9303-3).
25. Malti, A.; Edberg, J.; Granberg, H.; Khan, Z. U.; Andreasen, J. W.; Liu, X.; Zhao, D.; Zhang, H.; Yao, Y.; Brill, J. W.; et al. An Organic Mixed Ion–Electron Conductor for Power Electronics. *Adv Sci (Weinh)* **2016**, *3*, 1500305. DOI: [10.1002/advs.201500305](https://doi.org/10.1002/advs.201500305).
26. Lay, M.; Pèlach, M. À.; Pellicer, N.; Tarrés, J. A.; Bun, K. N.; Vilaseca, F. Smart Nanopaper Based on Cellulose Nanofibers with Hybrid PEDOT:PSS/Polypyrrole for Energy Storage Devices. *Carbohydr. Polym.* **2017**, *165*, 86–95. DOI: [10.1016/j.carbpol.2017.02.043](https://doi.org/10.1016/j.carbpol.2017.02.043).
27. Say, M. G.; Brooke, R.; Edberg, J.; Grimoldi, A.; Belaineh, D.; Engquist, I.; Berggren, M. Spray-Coated Paper Supercapacitors. *NPJ Flex. Electron.* **2020**, *4*, 14. DOI: [10.1038/s41528-020-0079-8](https://doi.org/10.1038/s41528-020-0079-8).



28. Du, X.; Zhang, Z.; Liu, W.; Deng, Y. Nanocellulose-Based Conductive Materials and Their Emerging Applications in Energy devices - A Review. *Nano Energy* **2017**, *35*, 299–320. DOI: [10.1016/j.nanoen.2017.04.001](https://doi.org/10.1016/j.nanoen.2017.04.001).
29. Fang, Z.; Hou, G.; Chen, C.; Hu, L. Nanocellulose-Based Films and Their Emerging Applications. *Curr. Opin. Solid State Mater. Sci.* **2019**, *23*, 100764–100764. DOI: [10.1016/j.cossms.2019.07.003](https://doi.org/10.1016/j.cossms.2019.07.003).
30. Stríteský, S.; Marková, A.; Víteček, J.; Šafaříková, E.; Hrabal, M.; Kubáč, L.; Kubala, L.; Weiter, M.; Vala, M. Printing Inks of Electroactive Polymer PEDOT:PSS: The Study of Biocompatibility, Stability, and Electrical Properties. *J. Biomed. Mater. Res. A* **2018**, *106*, 1121–1128. DOI: [10.1002/jbm.a.36314](https://doi.org/10.1002/jbm.a.36314).
31. Wang, W. C.; Cheng, Y. T.; Estroff, B. Electrostatic Self-Assembly of Composite Nanofiber Yarn. *Polymers* **2020**, *13*, 12–19. DOI: [10.3390/polym13010012](https://doi.org/10.3390/polym13010012).
32. Kargarzadeh, H.; Mariano, M.; Gopakumar, D.; Ahmad, I.; Thomas, S.; Dufresne, A.; Huang, J.; Lin, N. *Advances in Cellulose Nanomaterials*. Vol. 25; Springer Netherlands: Dordrecht, Netherlands, **2018**; pp 2151–2189. DOI: [10.1007/s10570-018-1723-5](https://doi.org/10.1007/s10570-018-1723-5).
33. Bayer, T.; Cunning, B. V.; Šmíd, B.; Selyanchyn, R.; Fujikawa, S.; Sasaki, K.; Lyth, S. M. Spray Deposition of Sulfonated Cellulose Nanofibers as Electrolyte Membranes in Fuel Cells. *Cellulose* **2021**, *28*, 1355–1367. DOI: [10.1007/s10570-020-03593-w](https://doi.org/10.1007/s10570-020-03593-w).
34. Li, J.; Li, J.; Feng, D.; Zhao, J.; Sun, J.; Li, D. Excellent Rheological Performance and Impact Toughness of Cellulose Nanofibers/PLA/Ionomer Composite. *RSC Adv.* **2017**, *7*, 28889–28897. DOI: [10.1039/C7RA04302C](https://doi.org/10.1039/C7RA04302C).
35. Lay, M.; González, I.; Tarrés, J. A.; Pellicer, N.; Bun, K. N.; Vilaseca, F. High Electrical and Electrochemical Properties in Bacterial Cellulose/Polypyrrole Membranes. *Eur. Polym. J.* **2017**, *91*, 1–9. DOI: [10.1016/j.eurpolymj.2017.03.021](https://doi.org/10.1016/j.eurpolymj.2017.03.021).
36. Belaine, D.; Andreasen, J. W.; Palisaitis, J.; Malti, A.; Håkansson, K.; Wågberg, L.; Crispin, X.; Engquist, I.; Berggren, M. Controlling the Organization of PEDOT:PSS on Cellulose Structures. *ACS Appl. Polym. Mater.* **2019**, *1*, 2342–2351. DOI: [10.1021/acsapm.9b00444](https://doi.org/10.1021/acsapm.9b00444).
37. Nascimento, D. M.; Nunes, Y. L.; Figueirêdo, M. C. B.; de Azeredo, H. M. C.; Aouada, F. A.; Feitosa, J. P. A.; Rosa, M. F.; Dufresne, A. Nanocellulose Nanocomposite Hydrogels: Technological and Environmental Issues. *Green Chem.* **2018**, *20*, 2428–2448. DOI: [10.1039/C8GC00205C](https://doi.org/10.1039/C8GC00205C).
38. Lin, N.; Dufresne, A. Nanocellulose in Biomedicine: Current Status and Future Prospect. *Eur. Polym. J.* **2014**, *59*, 302–325. DOI: [10.1016/j.eurpolymj.2014.07.025](https://doi.org/10.1016/j.eurpolymj.2014.07.025).
39. Habibi, Y.; Lucia, L. A.; Rojas, O. J. Cellulose Nanocrystals: Chemistry, Self-Assembly, and Applications. *Chem. Rev.* **2010**, *110*, 3479–3500. DOI: [10.1021/cr900339w](https://doi.org/10.1021/cr900339w).
40. De France, K. J.; Hoare, T.; Cranston, E. D. Review of Hydrogels and Aerogels Containing Nanocellulose. *Chem. Mater.* **2017**, *29*, 4609–4631. DOI: [10.1021/acs.chemmater.7b00531](https://doi.org/10.1021/acs.chemmater.7b00531).
41. de Amorim, J. D. P.; de Souza, K. C.; Duarte, C. R.; da Silva Duarte, I.; de Assis Sales Ribeiro, F.; Silva, G. S.; de Farias, P. M. A.; Stingl, A.; Costa, A. F. S.; Vinhas, G. M.; et al. Plant and Bacterial Nanocellulose: Production, Properties and Applications in Medicine, Food, Cosmetics, Electronics and Engineering. A Review. *Environ. Chem. Lett.* **2020**, *18*, 851–869. DOI: [10.1007/s10311-020-00989-9](https://doi.org/10.1007/s10311-020-00989-9).
42. Fry, S. C. Plant Cell Walls. From Chemistry to Biology. *Ann. Bot.* **2011**, *108*, viii–viix. DOI: [10.1093/aob/mcr128](https://doi.org/10.1093/aob/mcr128).
43. Larsson, P. A.; Riazanova, A. V.; Cinar Ciftci, G.; Rojas, R.; Øvrebø, H. H.; Wågberg, L.; Berglund, L. A. Towards Optimised Size Distribution in Commercial Microfibrillated Cellulose: A Fractionation Approach. *Cellulose* **2019**, *26*, 1565–1575. DOI: [10.1007/s10570-018-2214-4](https://doi.org/10.1007/s10570-018-2214-4).
44. Li, T.; Chen, C.; Brozena, A. H.; Zhu, J. Y.; Xu, L.; Driemeier, C.; Dai, J.; Rojas, O. J.; Isogai, A.; Wågberg, L.; et al. Developing Fibrillated Cellulose as a Sustainable Technological Material. *Nature* **2021**, *590*, 47–56. DOI: [10.1038/s41586-020-03167-7](https://doi.org/10.1038/s41586-020-03167-7).

45. Stelte, W.; Sanadi, A. R. Preparation and Characterization of Cellulose Nanofibers from Two Commercial Hardwood and Softwood Pulps. *Ind. Eng. Chem. Res.* **2009**, *48*, 11211–11219. DOI: [10.1021/ie9011672](https://doi.org/10.1021/ie9011672).
46. Nehra, P.; Chauhan, R. P. Eco-Friendly Nanocellulose and Its Biomedical Applications: Current Status and Future Prospect. *J. Biomater. Sci. Polym. Ed.* **2021**, *32*, 112–149. DOI: [10.1080/09205063.2020.1817706](https://doi.org/10.1080/09205063.2020.1817706).
47. Usov, I.; Nyström, G.; Adamcik, J.; Handschin, S.; Schütz, C.; Fall, A.; Bergström, L.; Mezzenga, R. Understanding Nanocellulose Chirality and Structure–Properties Relationship at the Single Fibril Level. *Nat. Commun.* **2015**, *6*, 7564. DOI: [10.1038/ncomms8564](https://doi.org/10.1038/ncomms8564).
48. Dourado, F.; Fontão, A. I.; Leal, M.; Rodrigues, A. C.; Gama, M. In *Process Modelling and Techno-Economic Evaluation of an Industrial Airlift Bacterial Cellulose Fermentation Process*; Lee, K.-Y. Ed.; CRC Press: Boca Raton, FL, **2018**; p 1–16.
49. Moon, S. M.; Heo, J. E.; Jeon, J.; Eom, T.; Jang, D.; Her, K.; Cho, W.; Woo, K.; Wie, J. J.; Shim, B. S. High Crystallinity of Tunicate Cellulose Nanofibers for High-Performance Engineering Films. *Carbohydr. Polym.* **2021**, *254*, 117470–117470. DOI: [10.1016/j.carbpol.2020.117470](https://doi.org/10.1016/j.carbpol.2020.117470).
50. Vicente, A. T.; Araújo, A.; Mendes, M. J.; Nunes, D.; Oliveira, M. J.; Sanchez-Sobrado, O.; Ferreira, M. P.; Águas, H.; Fortunato E.; Martins, R. Multifunctional Cellulose-Paper for Light Harvesting and Smart Sensing Applications. *J. Mater. Chem. C* **2018**, *6*, 3143–3181. DOI: [10.1039/C7TC05271](https://doi.org/10.1039/C7TC05271).
51. Zinge, C.; Kandasubramanian, B. Nanocellulose Based Biodegradable Polymers. *Eur. Polym. J.* **2020**, *133*, 109758–109758. DOI: [10.1016/j.eurpolymj.2020.109758](https://doi.org/10.1016/j.eurpolymj.2020.109758).
52. Heise, K.; Kontturi, E.; Allahverdiyeva, Y.; Tammelin, T.; Linder, M. B.; Ikkala, O. Nanocellulose: Recent Fundamental Advances and Emerging Biological and Biomimicking Applications. *Adv. Mater.* **2021**, *33*, 2004349. DOI: [10.1002/adma.202004349](https://doi.org/10.1002/adma.202004349).
53. Huang, J.; Ma, X.; Yang, G.; Alain, D. Introduction to Nanocellulose. In *Nanocellulose*; Huang, J., Dufresne, A., Lin, N. Eds.; Wiley-VCH Verlag GmbH & Co. KGaA: Weinheim, Germany, **2019**; pp 1–20.
54. Rietzler, B.; Ek, M. Adding Value to Spruce Bark by the Isolation of Nanocellulose in a Biorefinery Concept. *ACS Sustain. Chem. Eng.* **2021**, *9*, 1398–1405. DOI: [10.1021/acsschemeng.0c08429](https://doi.org/10.1021/acsschemeng.0c08429).
55. Yang, X.; Biswas, S. K.; Han, J.; Tanpichai, S.; Li, M.; Chen, C.; Zhu, S.; Das, A. K.; Yano, H. Surface and Interface Engineering for Nanocellulosic Advanced Materials. *Adv. Mater.* **2021**, *33*, 2002264. DOI: [10.1002/adma.202002264](https://doi.org/10.1002/adma.202002264).
56. Santmartí, A.; Lee, K.-Y. Crystallinity and Thermal Stability of Nanocellulose. In *Nanocellulose and Sustainability*; Lee, K.-Y. Ed.; New York, NY, **2018**; pp 67–86.
57. Cinar Ciftci, G.; Larsson, P. A.; Riazanova, A. V.; Øvrebø, H. H.; Wågberg, L.; Berglund, L. A. Tailoring of Rheological Properties and Structural Polydispersity Effects in Microfibrillated Cellulose Suspensions. *Cellulose* **2020**, *27*, 9227–9241. DOI: [10.1007/s10570-020-03438-6](https://doi.org/10.1007/s10570-020-03438-6).
58. Banvillet, G.; Gatt, E.; Belgacem, N.; Bras, J. Cellulose Fibers Deconstruction by Twin-Screw Extrusion with in Situ Enzymatic Hydrolysis via Bioextrusion. *Bioresour. Technol.* **2021**, *327*, 124819–124819. DOI: [10.1016/j.biortech.2021.124819](https://doi.org/10.1016/j.biortech.2021.124819).
59. Isogai, A. Emerging Nanocellulose Technologies: Recent Developments. *Adv. Mater.* **2021**, *33*, 2000630–2000610. DOI: [10.1002/adma.202000630](https://doi.org/10.1002/adma.202000630).
60. Koga, H.; Saito, T.; Kitaoka, T.; Nogi, M.; Suganuma, K.; Isogai, A. Transparent, Conductive, and Printable Composites Consisting of TEMPO-Oxidized Nanocellulose and Carbon Nanotube. *Biomacromolecules* **2013**, *14*, 1160–1165. DOI: [10.1021/bm400075f](https://doi.org/10.1021/bm400075f).
61. Saito, T.; Okita, Y.; Nge, T. T.; Sugiyama, J.; Isogai, A. TEMPO-Mediated Oxidation of Native Cellulose: Microscopic Analysis of Fibrous Fractions in the Oxidized Products. *Carbohydr. Polym.* **2006**, *65*, 435–440. DOI: [10.1016/j.carbpol.2006.01.034](https://doi.org/10.1016/j.carbpol.2006.01.034).

62. Kádár, R.; Spirk, S.; Nypelö, T. Cellulose Nanocrystal Liquid Crystal Phases: Progress and Challenges in Characterization Using Rheology Coupled to Optics, Scattering, and Spectroscopy. *ACS Nano*. **2021**, *15*, 7931–7945. DOI: [10.1021/acsnano.0c09829](https://doi.org/10.1021/acsnano.0c09829).
63. Abitbol, T.; Kloser, E.; Gray, D. G. Estimation of the Surface Sulfur Content of Cellulose Nanocrystals Prepared by Sulfuric Acid Hydrolysis. *Cellulose* **2013**, *20*, 785–794. DOI: [10.1007/s10570-013-9871-0](https://doi.org/10.1007/s10570-013-9871-0).
64. Czaja, W. K.; Young, D. J.; Kawecki, M.; Brown, R. M. The Future Prospects of Microbial Cellulose in Biomedical Applications. *Biomacromolecules* **2007**, *8*, 1–12. DOI: [10.1021/bm060620d](https://doi.org/10.1021/bm060620d).
65. Zhong, C. Industrial-Scale Production and Applications of Bacterial Cellulose. *Front. Bioeng. Biotechnol.* **2020**, *8*, 1–19. DOI: [10.3389/fbioe.2020.605374](https://doi.org/10.3389/fbioe.2020.605374).
66. Ullah, M. W.; Manan, S.; Kiprono, S. J.; Ul-Islam, M.; Yang, G. Synthesis, Structure, and Properties of Bacterial Cellulose. In *Nanocellulose*; Huang, J.; Dufresne, A.; Lin, N.; Eds. Wiley Online Library. **2019**. Doi: [10.1002/9783527807437.ch4](https://doi.org/10.1002/9783527807437.ch4).
67. Abol-Fotouh, D.; Hassan, M. A.; Shokry, H.; Roig, A.; Azab, M. S.; Kashyout, A. E.-H. B. Bacterial Nanocellulose from Agro-Industrial Wastes: Low-Cost and Enhanced Production by *Komagataeibacter saccharivorans* MD1. *Sci. Rep.* **2020**, *10*, 1–14. DOI: [10.1038/s41598-020-60315-9](https://doi.org/10.1038/s41598-020-60315-9).
68. Kaushik, M.; Moores, A. Review: Nanocelluloses as Versatile Supports for Metal Nanoparticles and Their Applications in Catalysis. *Green Chem.* **2016**, *18*, 622–637. DOI: [10.1039/C5GC02500A](https://doi.org/10.1039/C5GC02500A).
69. Miyashiro, D.; Hamano, R.; Umemura, K. A Review of Applications Using Mixed Materials of Cellulose, Nanocellulose and Carbon Nanotubes. *Nanomaterials* **2020**, *10*, 186. DOI: [10.3390/nano10020186](https://doi.org/10.3390/nano10020186).
70. Aleshin, A. N.; Williams, S. R.; Heeger, A. J. Transport Properties of Poly (3,4-Ethylenedioxythiophene)/Poly (Styrenesulfonate). *Synth. Met.* **1998**, *94*, 173–177. DOI: [10.1016/S0379-6779\(97\)04167-2](https://doi.org/10.1016/S0379-6779(97)04167-2).
71. Naveen, M. H.; Gurudatt, N. G.; Shim, Y.-B. Applications of Conducting Polymer Composites to Electrochemical Sensors: A Review. *Appl. Mater. Today* **2017**, *9*, 419–433. DOI: [10.1016/j.apmt.2017.09.001](https://doi.org/10.1016/j.apmt.2017.09.001).
72. Gueye, M. N.; Carella, A.; Faure-Vincent, J.; Demadrille, R.; Simonato, J.-P. Progress in Understanding Structure and Transport Properties of PEDOT-Based Materials: A Critical Review. *Prog. Mater. Sci.* **2020**, *108*, 100616–100616. DOI: [10.1016/j.pmatsci.2019.100616](https://doi.org/10.1016/j.pmatsci.2019.100616).
73. Brooke, R.; Cottis, P.; Talemi, P.; Fabretto, M.; Murphy, P.; Evans, D. Recent Advances in the Synthesis of Conducting Polymers from the Vapour Phase. *Prog. Mater. Sci.* **2017**, *86*, 127–146. DOI: [10.1016/j.pmatsci.2017.01.004](https://doi.org/10.1016/j.pmatsci.2017.01.004).
74. Hu, L.; Song, J.; Yin, X.; Su, Z.; Li, Z. Research Progress on Polymer Solar Cells Based on PEDOT: PSS Electrodes. *Polymers* **2020**, *12*, 145. DOI: [10.3390/polym12010145](https://doi.org/10.3390/polym12010145).
75. Yang, Y.; Deng, H.; Fu, Q. Recent Progress on PEDOT: PSS Based Polymer Blends and Composites for Flexible Electronics and Thermoelectric Devices. *Mater. Chem. Front.* **2020**, *4*, 3130–3152. DOI: [10.1039/D0QM00308E](https://doi.org/10.1039/D0QM00308E).
76. Fabretto, M. V.; Evans, D. R.; Mueller, M.; Zuber, K.; Hojati-Talemi, P.; Short, R. D.; Wallace, G. G.; Murphy, P. J. Polymeric Material with Metal-Like Conductivity for Next Generation Organic Electronic Devices. *Chem. Mater.* **2012**, *24*, 3998–4003. DOI: [10.1021/cm302899v](https://doi.org/10.1021/cm302899v).
77. Bubnova, O.; Khan, Z. U.; Wang, H.; Braun, S.; Evans, D. R.; Fabretto, M.; Hojati-Talemi, P.; Dagnelund, D.; Arlin, J.-B.; Geerts, Y. H.; et al. Semi-Metallic Polymers. *Nat. Mater.* **2014**, *13*, 190–194. DOI: [10.1038/nmat3824](https://doi.org/10.1038/nmat3824).
78. Edberg, J.; Iandolo, D.; Brooke, R.; Liu, X.; Musumeci, C.; Andreasen, J. W.; Simon, D. T.; Evans, D.; Engquist, I.; Berggren, M. Patterning and Conductivity Modulation of Conductive Polymers by UV Light Exposure. *Adv. Funct. Mater.* **2016**, *26*, 6950–6960. DOI: [10.1002/adfm.201601794](https://doi.org/10.1002/adfm.201601794).

79. Wei, T. C.; Chen, S. H.; Chen, C. Y. Highly Conductive PEDOT:PSS Film Made with Ethylene-Glycol Addition and Heated-Stir Treatment for Enhanced Photovoltaic Performances. *Mater. Chem. Front.* **2020**, *4*, 3302–3309. DOI: [10.1039/D0QM00529K](https://doi.org/10.1039/D0QM00529K).
80. Sun, K.; Zhang, S.; Li, P.; Xia, Y.; Zhang, X.; Du, D.; Isikgor, F. H.; Ouyang, J. Review on Application of PEDOTs and PEDOT:PSS in Energy Conversion and Storage Devices. *J. Mater. Sci. Mater. Electron.* **2015**, *26*, 4438–4462. DOI: [10.1007/s10854-015-2895-5](https://doi.org/10.1007/s10854-015-2895-5).
81. Han, Y. Enhanced Electrical Properties of PEDOT:PSS via Synergistic Effect. *Soft Mater.* **2018**, *16*, 31–36. DOI: [10.1080/1539445X.2017.1387151](https://doi.org/10.1080/1539445X.2017.1387151).
82. Wen, N.; Fan, Z.; Yang, S.; Zhao, Y.; Cong, T.; Xu, S.; Zhang, H.; Wang, J.; Huang, H.; Li, C.; et al. Highly Conductive, Ultra-Flexible and Continuously Processable PEDOT:PSS Fibers with High Thermoelectric Properties for Wearable Energy Harvesting. *Nano Energy* **2020**, *78*, 105361–105361. DOI: [10.1016/j.nanoen.2020.105361](https://doi.org/10.1016/j.nanoen.2020.105361).
83. Zhou, S.; Qiu, Z.; Strömme, M.; Wang, Z. Highly Crystalline PEDOT Nanofiber Templated by Highly Crystalline Nanocellulose. *Adv. Funct. Mater.* **2020**, *30*, 2005757–2005759. DOI: [10.1002/adfm.202005757](https://doi.org/10.1002/adfm.202005757).
84. Dong, J.; Portale, G. Role of the Processing Solvent on the Electrical Conductivity of PEDOT:PSS. *Adv. Mater. Interfaces* **2020**, *7*, 2000641. DOI: [10.1002/admi.202000641](https://doi.org/10.1002/admi.202000641).
85. Kee, S.; Kim, N.; Park, H.; Kim, B. S.; Teo, M. Y.; Lee, S.; Kim, J.; Lee, K. Tuning the Mechanical and Electrical Properties of Stretchable PEDOT:PSS/Ionic Liquid Conductors. *Macromol. Chem. Phys.* **2020**, *221*, 2000291–2000298. DOI: [10.1002/macp.202000291](https://doi.org/10.1002/macp.202000291).
86. Bae, E. J.; Kang, Y. H.; Jang, K.-S.; Cho, S. Y. Enhancement of Thermoelectric Properties of PEDOT:PSS and Tellurium-PEDOT:PSS Hybrid Composites by Simple Chemical Treatment. *Sci. Rep.* **2016**, *6*, 18805–18810. DOI: [10.1038/srep18805](https://doi.org/10.1038/srep18805).
87. Zhou, J.; Kimura, M. Electromechanical Actuation of Highly Conductive PEDOT/PSS-Coated Cellulose Papers. *Sen-i. Gakkaishi* **2011**, *67*, 125–131. DOI: [10.2115/fiber.67.125](https://doi.org/10.2115/fiber.67.125).
88. Kim, S.-S.; Jeon, J.-H.; Kee, C.-D.; Oh, I.-K. Electro-Active Hybrid Actuators Based on Freeze-Dried Bacterial Cellulose and PEDOT:PSS. *Smart Mater. Struct.* **2013**, *22*, 085026. DOI: [10.1088/0964-1726/22/8/085026](https://doi.org/10.1088/0964-1726/22/8/085026).
89. Malti, A.; Brooke, R.; Liu, X.; Zhao, D.; Andersson Ersman, P.; Fahlman, M.; Jonsson, M. P.; Berggren, M.; Crispin, X. Freestanding Electrochromic Paper. *J. Mater. Chem. C* **2016**, *4*, 9680–9686. DOI: [10.1039/C6TC03542F](https://doi.org/10.1039/C6TC03542F).
90. Basavaraja, C.; Park, J. Y.; Huh, D. S. Degradable and Electrically Conductive Poly(3,4-Ethylenedioxythiophene)/Sigma Cell Cellulose Polymer Composites. *Polym. Compos.* **2017**, *38*, 1864–1872. DOI: [10.1002/pc.23756](https://doi.org/10.1002/pc.23756).
91. Han, S.; Jiao, F.; Khan, Z. U.; Edberg, J.; Fabiano, S.; Crispin, X. Thermoelectric Polymer Aerogels for Pressure–Temperature Sensing Applications. *Adv. Funct. Mater.* **2017**, *27*, 1703549. DOI: [10.1002/adfm.201703549](https://doi.org/10.1002/adfm.201703549).
92. Edberg, J.; Inganäs, O.; Engquist, I.; Berggren, M. Boosting the Capacity of All-Organic Paper Supercapacitors Using Wood Derivatives. *J. Mater. Chem. A* **2018**, *6*, 145–152. DOI: [10.1039/C7TA06810G](https://doi.org/10.1039/C7TA06810G).
93. Jain, K.; Reid, M. S.; Larsson, P. A.; Wågberg, L. On the Interaction between PEDOT:PSS and Cellulose: Adsorption Mechanisms and Controlling Factors. *Carbohydr. Polym.* **2021**, *260*, 117818. DOI: [10.1016/j.carbpol.2021.117818](https://doi.org/10.1016/j.carbpol.2021.117818).
94. Latonen, R.-M.; Cabrera, J. A. W.; Lund, S.; Kosourov, S.; Vajravel, S.; Boeva, Z.; Wang, X.; Xu, C.; Allahverdiyeva, Y. Electrospinning of Electroconductive Water-Resistant Nanofibers of PEDOT-PSS, Cellulose Nanofibrils and PEO: Fabrication, Characterization, and Cytocompatibility. *ACS Appl. Bio Mater.* **2021**, *4*, 483–493. DOI: [10.1021/acsabm.0c00989](https://doi.org/10.1021/acsabm.0c00989).
95. Feng, X.; Wang, X.; Wang, M.; Zhou, S.; Dang, C.; Zhang, C.; Chen, Y.; Qi, H. Novel PEDOT Dispersion by in-Situ Polymerization Based on Sulfated Nanocellulose. *Chem. Eng. J.* **2021**, *418*, 129533. DOI: [10.1016/j.cej.2021.129533](https://doi.org/10.1016/j.cej.2021.129533).
96. Lars, W.; Lars, O. Polymer Adsorption on Cellulosic Fibers. *Nordic Pulp Paper Res. J.* **1989**, *4*, 135–140. DOI: [10.3183/npprj-1989-04-02-p135-140](https://doi.org/10.3183/npprj-1989-04-02-p135-140).

97. Edberg, J.; Malti, A.; Granberg, H.; Hamed, M. M.; Crispin, X.; Engquist, I.; Berggren, M. Electrochemical Circuits from 'Cut and Stick' PEDOT:PSS-Nanocellulose Composite. *Flex. Print. Electron.* **2017**, *2*, 045010. DOI: [10.1088/2058-8585/aa8027](https://doi.org/10.1088/2058-8585/aa8027).
98. Wang, X.; Grimoldi, A.; Håkansson, K.; Fall, A.; Granberg, H.; Mengistie, D.; Edberg, J.; Engquist, I.; Nilsson, D.; Berggren, M.; et al. Anisotropic Conductivity of Cellulose-PEDOT:PSS Composite Materials Studied with a Generic 3D Four-Point Probe Tool. *Org. Electron.* **2019**, *66*, 258–264. DOI: [10.1016/j.orgel.2018.12.023](https://doi.org/10.1016/j.orgel.2018.12.023).
99. Mehandezhiyski, A. Y.; Zozoulenko, I. Computational Microscopy of PEDOT:PSS/Cellulose Composite Paper. *ACS Appl. Energy Mater.* **2019**, *2*, 3568–3577. DOI: [10.1021/acsaem.9b00307](https://doi.org/10.1021/acsaem.9b00307).
100. Zhou, J.; Hsieh, Y.-L. Conductive Polymer Protonated Nanocellulose Aerogels for Tunable and Linearly Responsive Strain Sensors. *ACS Appl. Mater. Interfaces.* **2018**, *10*, 27902–27910. DOI: [10.1021/acsaami.8b10239](https://doi.org/10.1021/acsaami.8b10239).
101. Alam, K. M.; Kar, P.; Thakur, U. K.; Kisslinger, R.; Mahdi, N.; Mohammadpour, A.; Baheti P. A.; Kumar P.; Shankar, K. Remarkable Self-Organization and Unusual Conductivity Behavior in Cellulose nanocrystal-PEDOT: PSS Nanocomposites. *J. Mater. Sci. Mater. Electron.* **2019**, *30*, 1390–1399. DOI: [10.1007/s10854-018-0409-y](https://doi.org/10.1007/s10854-018-0409-y).
102. Medronho, B.; Romano, A.; Miguel, M. G.; Stigsson, L.; Lindman, B. Rationalizing Cellulose (in)Solubility: Reviewing Basic Physicochemical Aspects and Role of Hydrophobic Interactions. *Cellulose* **2012**, *19*, 581–587. DOI: [10.1007/s10570-011-9644-6](https://doi.org/10.1007/s10570-011-9644-6).
103. Kong, F.; Liu, C.; Song, H.; Xu, J.; Huang, Y.; Zhu, H.; Wang, J. Effect of Solution pH Value on Thermoelectric Performance of Free-Standing PEDOT:PSS Films. *Synth. Met.* **2013**, *185–186*, 31–37. DOI: [10.1016/j.synthmet.2013.09.046](https://doi.org/10.1016/j.synthmet.2013.09.046).
104. Mochizuki, Y.; Horii, T.; Okuzaki, H. Effect of pH on Structure and Conductivity of PEDOT/PSS. *Trans. Mat. Res. Soc. Japan* **2012**, *37*, 307–310. DOI: [10.14723/tmrsj.37.307](https://doi.org/10.14723/tmrsj.37.307).
105. Modarresi, M.; Franco-gonzalez, J. F.; Zozoulenko, I. Computational Microscopy Study of the Granular Structure and pH Dependence of PEDOT: PSS. *Phys. Chem. Chem. Phys.* **2019**, *21*, 34–36. DOI: [10.1039/C8CP07141A](https://doi.org/10.1039/C8CP07141A).
106. Brett, C. J.; Forslund, O. K.; Nocerino, E.; Kreuzer, L. P.; Widmann, T.; Porcar, L.; Yamada, N. L.; Matsubara, N.; Månsson, M.; Müller-Buschbaum, P.; et al. Humidity-Induced Nanoscale Restructuring in PEDOT:PSS and Cellulose Nanofibrils Reinforced Biobased Organic Electronics. *Adv. Electron. Mater.* **2021**, *7*, 2100137. DOI: [10.1002/aelm.202100137](https://doi.org/10.1002/aelm.202100137).
107. Chae, H.; Jung, M.; Cheong, H.; Soum, V.; Jo, S.; Kim, H.; Kim, T.; Kim, K.; Jeon, S.; Kwon, O. S.; Shin, K. Thermoelectric Temperature Sensors by Printing with a Simple Office Inkjet Printer. **2016**, *4*, 151–155. <https://briefs.techconnect.org/wp-content/volumes/TCB2016v4/pdf/911.pdf>
108. Terasawa, N.; Asaka, K. Self-Standing Cellulose Nanofiber/Poly(3,4-Ethylenedioxythiophene):Poly(4-Styrenesulfonate)/Ionic Liquid Actuators with Superior Performance. *RSC Adv.* **2018**, *8*, 33149–33155. DOI: [10.1039/c8ra06981f](https://doi.org/10.1039/c8ra06981f).
109. Brooke, R.; Edberg, J.; Say, M. G.; Sawatdee, A.; Grimoldi, A.; Åhlin, J.; Gustafsson, G.; Berggren, M.; Engquist, I. Supercapacitors on Demand: all-Printed Energy Storage Devices with Adaptable Design. *Flex. Print. Electron.* **2019**, *4*, 015006. DOI: [10.1088/2058-8585/aafc4f](https://doi.org/10.1088/2058-8585/aafc4f).
110. Inácio, P. M.; Medeiros, M. C.; Carvalho, T.; Félix, R. C.; Mestre, A.; Hubbard, P. C.; Ferreira, Q.; Morgado, J.; Charas, A.; Freire, C. S.; et al. Ultra-Low Noise PEDOT:PSS Electrodes on Bacterial Cellulose: A Sensor to Access Bioelectrical Signals in Non-Electrogenic Cells. *Org. Electron.* **2020**, *85*, 105882. DOI: [10.1016/j.orgel.2020.105882](https://doi.org/10.1016/j.orgel.2020.105882).
111. Wang, X.; Gao, K.; Shao, Z.; Peng, X.; Wu, X.; Wang, F. Layer-by-Layer Assembled Hybrid Multilayer Thin Film Electrodes Based on Transparent Cellulose Nanofibers Paper for Flexible Supercapacitors Applications. *J. Power Sources* **2014**, *249*, 148–155. DOI: [10.1016/j.jpowsour.2013.09.130](https://doi.org/10.1016/j.jpowsour.2013.09.130).

112. Ko, Y.; Kim, D.; Kim, U.-J.; You, J. Vacuum-Assisted Bilayer PEDOT:PSS/Cellulose Nanofiber Composite Film for Self-Standing, Flexible, Conductive Electrodes. *Carbohydr. Polym.* **2017**, *173*, 383–391. DOI: [10.1016/j.carbpol.2017.05.096](https://doi.org/10.1016/j.carbpol.2017.05.096).
113. Ravit, R.; Azman, N. H. N.; Kulandaivalu, S.; Abdullah, J.; Ahmad, I.; Sulaiman, Y. Cauliflower-like Poly(3,4-Ethylenedioxythiophene)/Nanocrystalline Cellulose/Manganese Oxide Ternary Nanocomposite for Supercapacitor. *J. Appl. Polym. Sci.* **2020**, *137*, 49162. DOI: [10.1002/app.49162](https://doi.org/10.1002/app.49162).
114. Ravit, R.; Abdullah, J.; Ahmad, I.; Sulaiman, Y. Electrochemical Performance of Poly(3, 4-Ethylenedioxythiophene)/Nanocrystalline Cellulose (PEDOT/NCC) Film for Supercapacitor. *Carbohydr. Polym.* **2019**, *203*, 128–138. DOI: [10.1016/j.carbpol.2018.09.043](https://doi.org/10.1016/j.carbpol.2018.09.043).
115. Jiao, F.; Edberg, J.; Zhao, D.; Puzinas, S.; Khan, Z. U.; Mäkie, P.; Naderi, A.; Lindström, T.; Odén, M.; Engquist, I.; et al. Nanofibrillated Cellulose-Based Electrolyte and Electrode for Paper-Based Supercapacitors. *Adv. Sustainable Syst.* **2018**, *2*, 1700121. DOI: [10.1002/adsu.201700121](https://doi.org/10.1002/adsu.201700121).
116. Rosén, T.; Hsiao, B. S.; Söderberg, L. D. Elucidating the Opportunities and Challenges for Nanocellulose Spinning. *Adv. Mater.* **2021**, *33*, 2001238. DOI: [10.1002/adma.202001238](https://doi.org/10.1002/adma.202001238).
117. Darabi, S.; Hummel, M.; Rantasalo, S.; Rissanen, M.; Öberg Månsson, I.; Hilke, H.; Hwang, B.; Skrifvars, M.; Hamed, M. M.; Sixta, H.; et al. Green Conducting Cellulose Yarns for Machine-Sewn Electronic Textiles. *ACS Appl. Mater. Interfaces.* **2020**, *12*, 56403–56412. DOI: [10.1021/acsami.0c15399](https://doi.org/10.1021/acsami.0c15399).
118. Zhang, J.; Seyedin, S.; Qin, S.; Lynch, P. A.; Wang, Z.; Yang, W.; Wang, X.; Razal, J. M. Fast and Scalable Wet-Spinning of Highly Conductive PEDOT:PSS Fibers Enables Versatile Applications. *J. Mater. Chem. A* **2019**, *7*, 6401–6410. DOI: [10.1039/C9TA00022D](https://doi.org/10.1039/C9TA00022D).
119. Sarabia-Riquelme, R.; Andrews, R.; Anthony, J. E.; Weisenberger, M. C. Highly Conductive Wet-Spun PEDOT:PSS Fibers for Applications in Electronic Textiles. *J. Mater. Chem. C* **2020**, *8*, 11618–11630. DOI: [10.1039/D0TC02558E](https://doi.org/10.1039/D0TC02558E).
120. Lim, T.; Kim, Y.; Jeong, S.-M.; Kim, C.-H.; Kim, S.-M.; Park, S. Y.; Yoon, M.-H.; Ju, S. Human Sweat Monitoring Using Polymer-Based Fiber. *Sci. Rep.* **2019**, *9*, 1–9. DOI: [10.1038/s41598-019-53677-2](https://doi.org/10.1038/s41598-019-53677-2).
121. Lund, A.; van der Velden, N. M.; Persson, N.-K.; Hamed, M. M.; Müller, C. Electrically Conducting Fibres for e-Textiles: An Open Playground for Conjugated Polymers and Carbon Nanomaterials. *Mater. Sci. Eng. R Rep.* **2018**, *126*, 1–29. DOI: [10.1016/j.mser.2018.03.001](https://doi.org/10.1016/j.mser.2018.03.001).
122. Ryan, J. D.; Mengistie, D. A.; Gabrielsson, R.; Lund, A.; Müller, C. Machine-Washable PEDOT:PSS Dyed Silk Yarns for Electronic Textiles. *ACS Appl. Mater. Interfaces.* **2017**, *9*, 9045–9050. DOI: [10.1021/acsami.7b00530](https://doi.org/10.1021/acsami.7b00530).
123. Gonçalves, C.; Ferreira da Silva, A.; Gomes, J.; Simoes, R. Wearable e-Textile Technologies: A Review on Sensors, Actuators and Control Elements. *Inventions* **2018**, *3*, 14–13. DOI: [10.3390/inventions3010014](https://doi.org/10.3390/inventions3010014).
124. Iwamoto, S.; Isogai, A.; Iwata, T. Structure and Mechanical Properties of Wet-Spun Fibers Made from Natural Cellulose Nanofibers. *Biomacromolecules* **2011**, *12*, 831–836. DOI: [10.1021/bm101510r](https://doi.org/10.1021/bm101510r).
125. Walther, A.; Timonen, J. V. I.; Díez, I.; Laukkanen, A.; Ikkala, O. Multifunctional High-Performance Biofibers Based on Wet-Extrusion of Renewable Native Cellulose Nanofibrils. *Adv. Mater.* **2011**, *23*, 2924–2928. DOI: [10.1002/adma.201100580](https://doi.org/10.1002/adma.201100580).
126. Håkansson, K. M. O.; Fall, A. B.; Lundell, F.; Yu, S.; Krywka, C.; Roth, S. V.; Santoro, G.; Kwick, M.; Prah Wittberg, L.; Wågberg, L.; et al. Hydrodynamic Alignment and Assembly of Nanofibrils Resulting in Strong Cellulose Filaments. *Nat. Commun.* **2014**, *5*, 4018. DOI: [10.1038/ncomms5018](https://doi.org/10.1038/ncomms5018).
127. Mittal, N.; Ansari, F.; Gowda V, K.; Brouzet, C.; Chen, P.; Larsson, P. T.; Roth, S. V.; Lundell, F.; Wågberg, L.; Kotov, N. A.; et al. Multiscale Control of Nanocellulose

- Assembly: Transferring Remarkable Nanoscale Fibril Mechanics to Macroscale Fibers. *ACS Nano*. **2018**, *12*, 6378–6388. DOI: [10.1021/acsnano.8b01084](https://doi.org/10.1021/acsnano.8b01084).
128. Wei, J.; Geng, S.; Hedlund, J.; Oksman, K. Lightweight, Flexible, and Multifunctional Anisotropic Nanocellulose-Based Aerogels for CO<sub>2</sub> Adsorption. *Cellulose* **2020**, *27*, 2695–2707. DOI: [10.1007/s10570-019-02935-7](https://doi.org/10.1007/s10570-019-02935-7).
129. Revin, V. V.; Nazarova, N. B.; Tsareva, E. E.; Liyaskina, E. V.; Revin, V. D.; Pestov, N. A. Production of Bacterial Cellulose Aerogels with Improved Physico-Mechanical Properties and Antibacterial Effect. *Front. Bioeng. Biotechnol.* **2020**, *8*, 1–19. DOI: [10.3389/fbioe.2020.603407](https://doi.org/10.3389/fbioe.2020.603407).
130. Sun, Y.; Chu, Y.; Wu, W.; Xiao, H. Nanocellulose-Based Lightweight Porous Materials: A Review. *Carbohydr. Polym.* **2021**, *255*, 117489–117489. DOI: [10.1016/j.carbpol.2020.117489](https://doi.org/10.1016/j.carbpol.2020.117489).
131. Françon, H.; Wang, Z.; Marais, A.; Mystek, K.; Piper, A.; Granberg, H.; Malti, A.; Gatenholm, P.; Larsson, P. A.; Wågberg, L.; et al. Ambient-Dried, 3D-Printable and Electrically Conducting Cellulose Nanofiber Aerogels by Inclusion of Functional Polymers. *Adv. Funct. Mater.* **2020**, *30*, 1909383. DOI: [10.1002/adfm.201909383](https://doi.org/10.1002/adfm.201909383).
132. Abdul Khalil, H. P. S.; Adnan, A. S.; Yahya, E. B.; Olaiya, N. G.; Safrida, S.; Hossain, M. S.; Balakrishnan, V.; Gopakumar, D. A.; Abdullah, C. K.; Oyekanmi, A. A.; et al. A Review on Plant Cellulose Nanofibre-Based Aerogels for Biomedical Applications. *Polymers* **2020**, *12*, 1759. DOI: [10.3390/polym12081759](https://doi.org/10.3390/polym12081759).
133. Chen, Y.; Zhang, L.; Yang, Y.; Pang, B.; Xu, W.; Duan, G.; Jiang, S.; Zhang, K. Recent Progress on Nanocellulose Aerogels: Preparation, Modification, Composite Fabrication, Applications. *Adv. Mater.* **2021**, *33*, 2005569. DOI: [10.1002/adma.202005569](https://doi.org/10.1002/adma.202005569).
134. Li, V. C. F.; Mulyadi, A.; Dunn, C. K.; Deng, Y.; Qi, H. J. Direct Ink Write 3D Printed Cellulose Nanofiber Aerogel Structures with Highly Deformable, Shape Recoverable, and Functionalizable Properties. *ACS Sustainable Chem. Eng.* **2018**, *6*, 2011–2022. DOI: [10.1021/acssuschemeng.7b03439](https://doi.org/10.1021/acssuschemeng.7b03439).
135. Han, S.; Alvi, N. U. H.; Granlöf, L.; Granberg, H.; Berggren, M.; Fabiano, S.; Crispin, X. A Multiparameter Pressure–Temperature–Humidity Sensor Based on Mixed Ionic–Electronic Cellulose Aerogels. *Adv. Sci. (Weinh)* **2019**, *6*, 1802128. DOI: [10.1002/advs.201802128](https://doi.org/10.1002/advs.201802128).
136. Han, S.; Ruoko, T.; Gladisch, J.; Erlandsson, J.; Wågberg, L.; Crispin, X.; Fabiano, S. Cellulose-Conducting Polymer Aerogels for Efficient Solar Steam Generation. *Adv. Sustainable Syst.* **2020**, *4*, 2000004. DOI: [10.1002/adsu.202000004](https://doi.org/10.1002/adsu.202000004).
137. Cheng, H.; Du, Y.; Wang, B.; Mao, Z.; Xu, H.; Zhang, L.; Zhong, Y.; Jiang, W.; Wang, L.; Sui, X.; et al. Flexible Cellulose-Based Thermoelectric Sponge towards Wearable Pressure Sensor and Energy Harvesting. *Chem. Eng. J.* **2018**, *338*, 1–7. DOI: [10.1016/j.cej.2017.12.134](https://doi.org/10.1016/j.cej.2017.12.134).
138. Hamedi, M.; Karabulut, E.; Marais, A.; Herland, A.; Nyström, G.; Wågberg, L. Nanocellulose Aerogels Functionalized by Rapid Layer-by-Layer Assembly for High Charge Storage and Beyond. *Angew. Chem. Int. Ed. Engl.* **2013**, *52*, 12038–12042. DOI: [10.1002/anie.201305137](https://doi.org/10.1002/anie.201305137).
139. Sai, T.; Fujita, K. A Review of Pulmonary Toxicity Studies of Nanocellulose. *Inhal. Toxicol.* **2020**, *32*, 231–239. DOI: [10.1080/08958378.2020.1770901](https://doi.org/10.1080/08958378.2020.1770901).
140. Trache, D.; Tarchoun, A. F.; Derradji, M.; Hamidon, T. S.; Masruchin, N.; Brosse, N.; Hussin, M. H. Nanocellulose: From Fundamentals to Advanced Applications. **2020**, *8*, 392. DOI: [10.3389/fchem.2020.00392](https://doi.org/10.3389/fchem.2020.00392).
141. Rajesh, M.; Raj, C. J.; Manikandan, R.; Kim, B. C.; Park, S. Y.; Yu, K. H. A High Performance PEDOT/PEDOT Symmetric Supercapacitor by Facile in-Situ Hydrothermal Polymerization of PEDOT Nanostructures on Flexible Carbon Fibre Cloth Electrodes. *Mater. Today Energy* **2017**, *6*, 96–104. DOI: [10.1016/j.mtener.2017.09.003](https://doi.org/10.1016/j.mtener.2017.09.003).
142. Wang, Z.; Tammela, P.; Huo, J.; Zhang, P.; Strømme, M.; Nyholm, L. Solution-Processed Poly(3,4-Ethylenedioxythiophene) Nanocomposite Paper Electrodes for High-Capacitance Flexible Supercapacitors. *J. Mater. Chem. A* **2016**, *4*, 1714–1722. DOI: [10.1039/C5TA10122K](https://doi.org/10.1039/C5TA10122K).

143. Sahalianov, I.; Say, M. G.; Abdullaeva, O. S.; Ahmed, F.; Glowacki, E.; Engquist, I.; Berggren, M.; Zozoulenko, I. Volumetric Double-Layer Charge Storage in Composites Based on Conducting Polymer PEDOT and Cellulose. *ACS Appl. Energy Mater.* **2021**, *4*, 8629–8640. DOI: [10.1021/acsaem.1c01850](https://doi.org/10.1021/acsaem.1c01850).
144. Anothumakkool, B.; Soni, R.; Bhange, S. N.; Kurungot, S. Novel Scalable Synthesis of Highly Conducting and Robust PEDOT Paper for a High Performance Flexible Solid Supercapacitor. *Energy Environ. Sci.* **2015**, *8*, 1339–1347. DOI: [10.1039/C5EE00142K](https://doi.org/10.1039/C5EE00142K).
145. Li, B.; Lopez-Beltran, H.; Siu, C.; Skorenko, K. H.; Zhou, H.; Bernier, W. E.; Whittingham, M. S.; Jones, W. E. Vapor Phase Polymerized PEDOT/Cellulose Paper Composite for Flexible Solid-State Supercapacitor. *ACS Appl. Energy Mater.* **2020**, *3*, 1559–1568. DOI: [10.1021/acsaem.9b02044](https://doi.org/10.1021/acsaem.9b02044).
146. Zhou, H.; Liu, G.; Liu, J.; Wang, Y.; Ai, Q.; Huang, J.; Yuan, Z.; Tan, L.; Chen, Y. Effective Network Formation of PEDOT by in-Situ Polymerization Using Novel Organic Template and Nanocomposite Supercapacitor. *Electrochim. Acta* **2017**, *247*, 871–879. DOI: [10.1016/j.electacta.2017.07.078](https://doi.org/10.1016/j.electacta.2017.07.078).
147. Kuang, Y.; Chen, C.; Pastel, G.; Li, Y.; Song, J.; Mi, R.; Kong, W.; Liu, B.; Jiang, Y.; Yang, K.; et al. Conductive Cellulose Nanofiber Enabled Thick Electrode for Compact and Flexible Energy Storage Devices. *Adv. Energy Mater.* **2018**, *8*, 1802398. DOI: [10.1002/aenm.201802398](https://doi.org/10.1002/aenm.201802398).
148. Edberg, J.; Brooke, R.; Granberg, H.; Engquist, I.; Berggren, M. Improving the Performance of Paper Supercapacitors Using Redox Molecules from Plants. *Adv. Sustain. Syst.* **2019**, *3*, 1900050. DOI: [10.1002/advsu.201900050](https://doi.org/10.1002/advsu.201900050).
149. Kurra, N.; Park, J.; Alshareef, H. N. A Conducting Polymer Nucleation Scheme for Efficient Solid-State Supercapacitors on Paper. *J. Mater. Chem. A* **2014**, *2*, 17058–17065. DOI: [10.1039/C4TA03603D](https://doi.org/10.1039/C4TA03603D).
150. Bu, Y.; Cao, M.; Jiang, Y.; Gao, L.; Shi, Z.; Xiao, X.; Wang, M.; Yang, G.; Zhou, Y.; Shen, Y.; et al. Ultra-Thin Bacterial Cellulose/Poly(Ethylenedioxythiophene) Nanofibers Paper Electrodes for All-Solid-State Flexible Supercapacitors. *Electrochim. Acta* **2018**, *271*, 624–631. DOI: [10.1016/j.electacta.2018.03.155](https://doi.org/10.1016/j.electacta.2018.03.155).
151. Ghosh, S.; Das, S.; Mosquera, M. E. G. Conducting Polymer-Based Nanohybrids for Fuel Cell Application. *Polymers* **2020**, *12*, 2993–2919. DOI: [10.3390/polym12122993](https://doi.org/10.3390/polym12122993).
152. Chen, C.; Kuang, Y.; Zhu, S.; Burgert, I.; Keplinger, T.; Gong, A.; Li, T.; Berglund, L.; Eichhorn, S. J.; Hu, L.; et al. Structure–Property–Function Relationships of Natural and Engineered Wood. *Nat. Rev. Mater.* **2020**, *5*, 642–666. DOI: [10.1038/s41578-020-0195-z](https://doi.org/10.1038/s41578-020-0195-z).
153. Vilela, C.; Morais, J. D.; Silva, A. C. Q.; Muñoz-Gil, D.; Figueiredo, F. M. L.; Silvestre, A. J. D.; Freire, C. S. R. Flexible Nanocellulose/Lignosulfonates Ion-Conducting Separators for Polymer Electrolyte Fuel Cells. *Nanomaterials (Basel)* **2020**, *10*, 1713. DOI: [10.3390/nano10091713](https://doi.org/10.3390/nano10091713).
154. Vilela, C.; Silvestre, A. J. D.; Figueiredo, F. M. L.; Freire, C. S. R. Nanocellulose-Based Materials as Components of Polymer Electrolyte Fuel Cells. *J. Mater. Chem. A* **2019**, *7*, 20045–20074. DOI: [10.1039/C9TA07466J](https://doi.org/10.1039/C9TA07466J).
155. Mitraga, E.; Vagin, M.; Sjöstedt, A.; Berggren, M.; Håkansson, K. M. O.; Jonsson, M. P.; Crispin, X. PEDOT-Cellulose Gas Diffusion Electrodes for Disposable Fuel Cells. *Adv. Sustainable Syst.* **2019**, *3*, 1900097–1900098. DOI: [10.1002/advsu.201900097](https://doi.org/10.1002/advsu.201900097).
156. Zhang, Q.; Sun, Y.; Xu, W.; Zhu, D. Organic Thermoelectric Materials: Emerging Green Energy Materials Converting Heat to Electricity Directly and Efficiently. *Adv. Mater.* **2014**, *26*, 6829–6851. DOI: [10.1002/adma.201305371](https://doi.org/10.1002/adma.201305371).
157. Zhang, L.; Shi, X.-L.; Yang, Y.-L.; Chen, Z.-G. Flexible Thermoelectric Materials and Devices: From Materials to Applications. *Mater. Today* **2021**, *46*, 62–108. DOI: [10.1016/j.mattod.2021.02.016](https://doi.org/10.1016/j.mattod.2021.02.016).
158. Xu, S.; Hong, M.; Shi, X.-L.; Wang, Y.; Ge, L.; Bai, Y.; Wang, L.; Dargusch, M.; Zou, J.; Chen, Z.-G.; et al. High-Performance PEDOT:PSS Flexible Thermoelectric Materials and Their Devices by Triple Post-Treatments. *Chem. Mater.* **2019**, *31*, 5238–5244. DOI: [10.1021/acs.chemmater.9b01500](https://doi.org/10.1021/acs.chemmater.9b01500).



159. Fan, Z.; Li, P.; Du, D.; Ouyang, J. Significantly Enhanced Thermoelectric Properties of PEDOT: PSS Films through Sequential Post-Treatments with Common Acids and Bases. *Adv. Sci. News* **2017**, *7*, 1602116–1602116. DOI: [10.1002/aenm.201602116](https://doi.org/10.1002/aenm.201602116).
160. Fan, Z.; Du, D.; Guan, X.; Ouyang, J. Polymer Films with Ultrahigh Thermoelectric Properties Arising from Significant Seebeck Coefficient Enhancement by Ion Accumulation on Surface. *Nano Energy* **2018**, *51*, 481–488. DOI: [10.1016/j.nanoen.2018.07.002](https://doi.org/10.1016/j.nanoen.2018.07.002).
161. Zhao, D.; Fabiano, S.; Berggren, M.; Crispin, X. Ionic Thermoelectric Gating Organic Transistors. *Nat. Commun.* **2017**, *8*, 14214. DOI: [10.1038/ncomms14214](https://doi.org/10.1038/ncomms14214).
162. Wang, H.; Zhao, D.; Khan, Z. U.; Puzinas, S.; Jonsson, M. P.; Berggren, M.; Crispin, X. Ionic Thermoelectric Figure of Merit for Charging of Supercapacitors. *Adv. Electron. Mater.* **2017**, *3*, 1700013. DOI: [10.1002/aelm.201700013](https://doi.org/10.1002/aelm.201700013).
163. Brill, J. W.; Shahi, M.; Payne, M. M.; Edberg, J.; Yao, Y.; Crispin, X.; Anthony, J. E. Frequency-Dependent Photothermal Measurement of Transverse Thermal Diffusivity of Organic Semiconductors. *J. Appl. Phys.* **2015**, *118*, 235501. DOI: [10.1063/1.4937565](https://doi.org/10.1063/1.4937565).
164. van de Ruit, K.; Katsouras, I.; Bollen, D.; van Mol, T.; Janssen, R. A. J.; de Leeuw, D. M.; Kemerink, M. The Curious Out-of-Plane Conductivity of PEDOT:PSS. *Adv. Funct. Mater.* **2013**, *23*, 5787–5793. DOI: [10.1002/adfm.201301175](https://doi.org/10.1002/adfm.201301175).
165. The international Energy Agency, Data and Statistics. **2021**. <https://www.iea.org/data-and-statistics?country=WORLD&fuel=Energy%20supply&indicator=CoalProdByType>.
166. Gao, L.; Chao, L.; Hou, M.; Liang, J.; Chen, Y.; Yu, H.-D.; Huang, W. Flexible, Transparent Nanocellulose Paper-Based Perovskite Solar Cells. *NPJ Flex. Electron.* **2019**, *3*, 4. DOI: [10.1038/s41528-019-0048-2](https://doi.org/10.1038/s41528-019-0048-2).
167. Méhes, G.; Vagin, M.; Mulla, M. Y.; Granberg, H.; Che, C.; Beni, V.; Crispin, X.; Berggren, M.; Stavrinidou, E.; Simon, D. T.; et al. Solar Heat-Enhanced Energy Conversion in Devices Based on Photosynthetic Membranes and PEDOT:PSS-Nanocellulose Electrodes. *Adv. Sustain. Syst.* **2020**, *4*, 1900100. DOI: [10.1002/advs.201900100](https://doi.org/10.1002/advs.201900100).
168. Liana, D. D.; Raguse, B.; Gooding, J. J.; Chow, E. Recent Advances in Paper-Based Sensors. *Sensors (Basel)* **2012**, *12*, 11505–11526. DOI: [10.3390/s120911505](https://doi.org/10.3390/s120911505).
169. Khiabani, P. S.; Soeriyadi, A. H.; Reece, P. J.; Gooding, J. J. Paper-Based Sensor for Monitoring Sun Exposure. *ACS Sens.* **2016**, *1*, 775–780. DOI: [10.1021/acssensors.6b00244](https://doi.org/10.1021/acssensors.6b00244).
170. Morais, R. M.; Klem, M. D. S.; Nogueira, G. L.; Gomes, T. C.; Alves, N. Low Cost Humidity Sensor Based on PANI/PEDOT:PSS Printed on Paper. *IEEE Sensors J.* **2018**, *18*, 2647–2651. DOI: [10.1109/JSEN.2018.2803018](https://doi.org/10.1109/JSEN.2018.2803018).
171. Ruecha, N.; Chailapakul, O.; Suzuki, K.; Citterio, D. Fully Inkjet-Printed Paper-Based Potentiometric Ion-Sensing Devices. *Anal. Chem.* **2017**, *89*, 10608–10616. DOI: [10.1021/acs.analchem.7b03177](https://doi.org/10.1021/acs.analchem.7b03177).
172. Khan, Z. U.; Edberg, J.; Hamed, M. M.; Gabrielsson, R.; Granberg, H.; Wågberg, L.; Engquist, I.; Berggren, M.; Crispin, X. Thermoelectric Polymers and Their Elastic Aerogels. *Adv. Mater.* **2016**, *28*, 4556–4562. DOI: [10.1002/adma.201505364](https://doi.org/10.1002/adma.201505364).
173. Kim, J.; Yun, S.; Mahadeva, S. K.; Yun, K.; Yang, S. Y.; Maniruzzaman, M. Paper Actuators Made with Cellulose and Hybrid Materials. *Sensors (Basel)* **2010**, *10*, 1473–1485. DOI: [10.3390/s100301473](https://doi.org/10.3390/s100301473).
174. Hamed, M. M.; Campbell, V. E.; Rothmund, P.; Güder, F.; Christodouleas, D. C.; Bloch, J.-F.; Whitesides, G. M. Electrically Activated Paper Actuators. *Adv. Funct. Mater.* **2016**, *26*, 2446–2453. DOI: [10.1002/adfm.201505123](https://doi.org/10.1002/adfm.201505123).
175. Mahadeva, S. K.; Kim, J. Effect of Polyelectrolyte Nanocoating on the Performance and Durability of Cellulose Electro-Active Paper Actuator. *J. Nanosci. Nanotechnol.* **2009**, *9*, 5757–5763. DOI: [10.1166/jnn.2009.1241](https://doi.org/10.1166/jnn.2009.1241).
176. Nan, M.; Wang, F.; Kim, S.; Li, H.; Jin, Z.; Bang, D.; Kim, C.-S.; Park, J.-O.; Choi, E. Ecofriendly High-Performance Ionic Soft Actuators Based on Graphene-Mediated Cellulose Acetate. *Sens. Actuators, B* **2019**, *301*, 127127. DOI: [10.1016/j.snb.2019.127127](https://doi.org/10.1016/j.snb.2019.127127).

177. Wang, F.; Jeon, J.-H.; Park, S.; Kee, C.-D.; Kim, S.-J.; Oh, I.-K. A Soft Biomolecule Actuator Based on a Highly Functionalized Bacterial Cellulose Nano-Fiber Network with Carboxylic Acid Groups. *Soft Matter*. **2016**, *12*, 246–254. DOI: [10.1039/c5sm00707k](https://doi.org/10.1039/c5sm00707k).
178. Terasawa, N. Effect of Ruthenium on Superior Performance of Cellulose Nanofibers/Poly(3,4-Ethylenedioxythiophene):Poly(4-Styrenesulfonate)/Ruthenium Oxide/Ionic Liquid Actuators. *Synth. Met.* **2020**, *261*, 116306. DOI: [10.1016/j.synthmet.2020.116306](https://doi.org/10.1016/j.synthmet.2020.116306).
179. Hu, F.; Xue, Y.; Xu, J.; Lu, B. PEDOT-Based Conducting Polymer Actuators. *Front. Robot. AI* **2019**, *6*, 114. DOI: [10.3389/frobt.2019.00114](https://doi.org/10.3389/frobt.2019.00114).
180. Helenius, G.; Bäckdahl, H.; Bodin, A.; Nannmark, U.; Gatenholm, P.; Risberg, B. In Vivo Biocompatibility of Bacterial Cellulose. *J. Biomed. Mater. Res. A* **2006**, *76*, 431–438. DOI: [10.1002/jbm.a.30570](https://doi.org/10.1002/jbm.a.30570).
181. Chen, C.; Zhang, T.; Zhang, Q.; Feng, Z.; Zhu, C.; Yu, Y.; Li, K.; Zhao, M.; Yang, J.; Liu, J.; et al. Three-Dimensional BC/PEDOT Composite Nanofibers with High Performance for Electrode–Cell Interface. *ACS Appl. Mater. Interfaces*. **2015**, *7*, 28244–28253. DOI: [10.1021/acsami.5b07273](https://doi.org/10.1021/acsami.5b07273).
182. Chen, C.; Yu, Y.; Li, K.; Zhao, M.; Liu, L.; Yang, J.; Liu, J.; Sun, D. Facile Approach to the Fabrication of 3D Electroconductive Nanofibers with Controlled Size and Conductivity Templated by Bacterial Cellulose. *Cellulose* **2015**, *22*, 3929–3939. DOI: [10.1007/s10570-015-0770-4](https://doi.org/10.1007/s10570-015-0770-4).
183. Chen, C.; Zhang, T.; Zhang, Q.; Chen, X.; Zhu, C.; Xu, Y.; Yang, J.; Liu, J.; Sun, D. Biointerface by Cell Growth on Graphene Oxide Doped Bacterial Cellulose/Poly(3,4-Ethylenedioxythiophene) Nanofibers. *ACS Appl. Mater. Interfaces*. **2016**, *8*, 10183–10192. DOI: [10.1021/acsami.6b01243](https://doi.org/10.1021/acsami.6b01243).
184. Fu, X.; Wang, J. K.; Ramírez-Pérez, A. C.; Choong, C.; Lisak, G. Flexible Conducting Polymer-Based Cellulose Substrates for on-Skin Applications. *Mater. Sci. Eng. C Mater. Biol. Appl.* **2020**, *108*, 110392. DOI: [10.1016/j.msec.2019.110392](https://doi.org/10.1016/j.msec.2019.110392).
185. Chen, C.; Chen, X.; Zhang, H.; Zhang, Q.; Wang, L.; Li, C.; Dai, B.; Yang, J.; Liu, J.; Sun, D.; et al. Electrically-Responsive Core-Shell Hybrid Microfibers for Controlled Drug Release and Cell Culture. *Acta Biomater.* **2017**, *55*, 434–442. DOI: [10.1016/j.actbio.2017.04.005](https://doi.org/10.1016/j.actbio.2017.04.005).